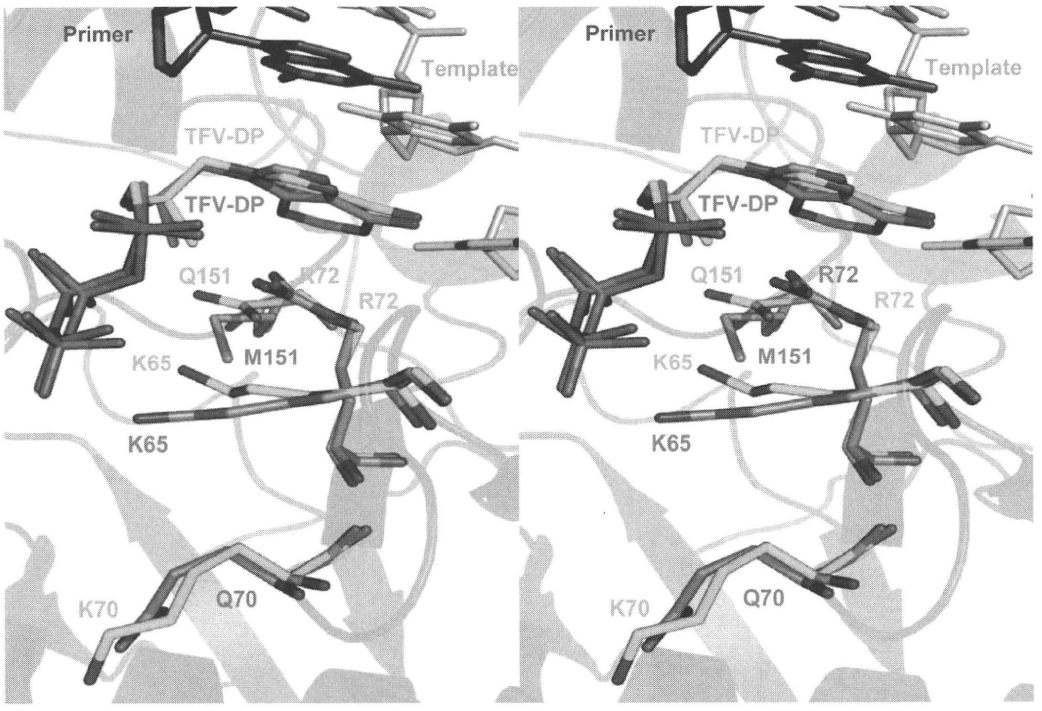

Figure 5. Stereo view of TFV-DP in the polymerase active site of WT RT and K70Q/Q151Mc RT. WT RT residues are shown as cyan sticks, K70Q/Q151Mc RT residues are shown as purple sticks. The primer strand is shown as dark gray sticks, template strand as light gray sticks. The fingers and palm subdomains are shown as blue and red cartoons, respectively.
doi:10.1371/journal.pone.0016242.g005

validation of contribution to resistance by using site-directed mutagenesis; 2) susceptibility testing of laboratory or clinical isolates; 3) nucleotide sequencing of viruses from patients in whom the drug is failing; 4) correlation studies between genotype at baseline and virologic response in patients exposed to a drug. Our study has unambiguously demonstrated that K70Q meets at least the first three criteria: evidence for criterion #1 is shown in Figure 2; for criterion #2 in Figures 1 and 2; and for criterion #3 in Figure 1 and Figure S1. Therefore, the K70Q mutation meets the criteria of a clinically relevant mutation.

In addition to the clinical and virological studies, we used biochemical techniques to determine the mechanism of TFV resistance imparted by the K70Q mutation to Q151Mc RTs. We used primer extension assays to show that K70Q/Q151Mc RT is less susceptible to TFV-DP than WT and Q151Mc RTs. We demonstrated that the mechanism of this resistance is not based on excision. On the contrary, we showed that the ATP-based excision of the mutant enzymes was slightly decreased with respect to WT RT, possibly because of decreased affinity of the mutant enzymes for the ATP excision substrate, incurred by changes in the binding environment of ATP, such as the loss of lysine at position 70.

Using transient-state kinetics we unambiguously established that the overall mechanism of K70Q/Q151Mc resistance to TFV is due to enhanced discrimination between the natural dATP substrate and TFV-DP. While all mutant enzymes had comparable efficiency of dATP incorporation, they displayed varying affinity and turnover rates of incorporation. It appears that the stronger effect of the enhanced discrimination overcomes the slight increase in sensitivity due to the small increase in excision. As a result, the mutant enzymes are resistant to the inhibitor.

Mutations at position 70 of RT have been known to confer NRTI resistance by two distinct mechanisms: K70R combined with at least two excision enhancing mutations, D67N and T215Y, enhances ATP-mediated excision of AZT and d4T [1,2,3,48] (*excision–dependent mechanism*). On the other hand, K70E causes resistance to 3TC, TFV, and ABC by lowering the maximum rate of inhibitor incorporation by RT (k_{pol}*-dependent exclusion mechanism*) [55]. Our results establish that in the background of Q151Mc, K70Q causes TFV resistance through a third mechanism: by decreasing the binding affinity of the inhibitor (K_d*-dependent exclusion mechanism*). Taken together, these findings highlight the remarkable ability of RT to use separate mutations at a single position to acquire NRTI resistance through three different mechanisms.

Our cell-based assays with infectious HIV-1 show that Q151Mc remains susceptible to TFV-DF, a finding consistent with previous reports [22]. Similarly, clinical isolates deposited at the Stanford HIV resistance database and carrying the Q151Mc mutation were also susceptible to TFV-DF, unless they also had the K65R mutation. However, pre-steady state characterization of TFV-DP incorporation by Q151Mc in this work (Table 2) and by others [59] showed that Q151Mc is less susceptible to TFV-DP than WT RT. This small discrepancy may be the result of potential differences in DNA-dependent and RNA-dependent DNA synthesis, or the result of the slightly increased excision of Q151Mc RT compared to WT RT (Fig. 3B and C).

To gain insights into the possible structural changes caused by the addition of K70Q to Q151Mc, we compared the molecular model of K70Q/Q151Mc RT/DNA/TFV-DP with the crystal structure of WT RT/DNA/TFV-DP [45] (Fig. 5). The network of hydrogen bonds involving the side-chains of K65, R72, and Q151 in the WT structure [26,27,54], is disrupted in the mutant structure. Also, Q151M and associated mutations A62V, V75I, and F77L are likely to modify the hydrophobic core of the fingers. We and others have previously shown that the side-chains of residues 72 and 65 interact with each other [35] and with Q151

and the α- and γ-phosphates of the incoming dNTP [26] or TFV-DP [45]. The functions of these residues have been established by several biochemical studies [21,25,60,61,62,63]. The reduction in polymerase rate (k_{pol}) and in binding affinity for TFV-DP (increased $K_{d,TFV\text{-}DP}$) may be the consequence of one or more such structural changes. Our molecular dynamics simulation experiments suggested a re-arrangement in the position of the side chain of K65, which is a catalytically important residue. While the precise effect of this change is not clear at this point, such changes could influence the overall binding of the substrate and/or the rate of nucleotide incorporation. Moreover, such movement of K65 in the presence of a mutation at position 70 is consistent with our previously reported crystallographic data, which established that there is an interplay between the positioning of the side chains at positions 70 and 65 [64]. Ongoing crystallographic studies are expected to provide more detailed structural insights into the role of K70Q in drug resistance.

In summary, we report here clinical data showing that addition of the K70Q mutation to the Q151Mc background confers high-level HIV resistance to TFV-DF and enhances resistance to other NRTIs. The biochemical mechanism of the TFV resistance is based on reduced binding affinity and incorporation of TFV-DP. Detection of this novel pattern of TFV-DF resistance may help adjust therapeutic regimens for the treatment of patients infected with multi-drug resistant HIV-1.

Supporting Information

Figure S1 Amino acid sequence alignment of the RT regions (amino acid 32 to 560) of the clinical isolates at time points 1 to 2 (see Figure 1A).
(DOC)

Figure S2 Effects of RT mutations K70Q, Q151Mc, or K70Q/Q151Mc on DNA primer extension activity and on ATP-based excision activities. (A) Effect of varying concentrations of TFV-DP on the primer extension activities of HIV-1 WT and mutant RTs. The experiments were carried out in the presence and absence of 3.5 mM ATP (marked as ATP (+) and ATP (−), respectively). Addition of ATP in the polymerization mixture allows measurement of the net sum of DNA polymerization and ATP-based excision activities. (B) Time dependence of ATP-based rescue of TFV-terminated primers. (C) ATP-based rescue was dependent on concentration of ATP.
(PPTX)

Figure S3 Pre-steady state incorporation of dATP or TFV-DP by K70Q and Q151Mc HIV-1 RTs. Single-nucleotide incorporation of dATP (panels A, B, and E) or TFV-DP (panels C, D, and F) by K70Q (panels A, C, E, and F) and Q151Mc (panels B, D, E, and F). Formation of extended primer products in the reactions with K70Q RT and Q151Mc RT were measured at 5 ms to 5 s time points, using the following dATP concentrations: 0.5 (■), 1 (□), 2.5 (▲), 5 (*), 10 (♦), 20 (◇), 50 (▼) and 75 μM (+). Incorporation of TFV was measured at 0.1–10 s reactions and at the following TFV-DP concentrations: 0.75 (■), 1.5 (□), 3.75 (▲), 7.5 (*), 15 (♦), 37.5 (◇) and 75 μM (▼) for reactions with K70Q RT (panel C), and 3.75 (▲), 7.5 (*), 37.5 (◇), 55 (▼), 75 (+) and 112.5 (•) for reactions with Q151Mc RT (panel D). (E) The amplitudes of the burst phases from the dATP reactions shown in panels A (K70Q, [▲]) and B (Q151Mc, [▼]) were plotted as a function of dATP concentrations. (F) The amplitudes of the burst phases from the TFV-DP reactions shown in panels C (K70Q, [▲]) and D (Q151Mc, [▼]) were plotted as a function of TFV-DP concentrations. The solid lines in panels A, B, C, and D represent the best fit of data to a burst equation. Each point represents average values of three experiments.
(PPTX)

Table S1 Drug susceptibility of clinical isolates.
(DOC)

Table S2 Drug susceptibility of HIV-1 variants carrying mutation at residue 70.
(DOC)

Table S3 Drug susceptibility of HIV-1 variants carrying mutation at residue 70 in the background of Q151M complex.
(DOC)

Acknowledgments

We thank Yukiko Takahashi and Fujie Negishi for sample preparation, and Dr. Hiroyuki Gatanaga and Dr. Michael A. Parniak for helpful discussions.

Author Contributions

Conceived and designed the experiments: AH ENK SO SGS. Performed the experiments: AH MMS KAK EM YS KS. Analyzed the data: AH MMS KAK KS SGS. Contributed reagents/materials/analysis tools: AH ENK SGS OS. Wrote the paper: AH ENK KS SGS.

References

1. Meyer PR, Matsuura SE, Mian AM, So AG, Scott WA (1999) A mechanism of AZT resistance: an increase in nucleotide-dependent primer unblocking by mutant HIV-1 reverse transcriptase. Mol Cell 4: 35–43.
2. Boyer PL, Sarafianos SG, Arnold E, Hughes SH (2001) Selective excision of AZTMP by drug-resistant human immunodeficiency virus reverse transcriptase. J Virol 75: 4832–4842.
3. Arion D, Kaushik N, McCormick S, Borkow G, Parniak MA (1998) Phenotypic mechanism of HIV-1 resistance to 3′-azido-3′-deoxythymidine (AZT): increased polymerization processivity and enhanced sensitivity to pyrophosphate of the mutant viral reverse transcriptase. Biochemistry 37: 15908–15917.
4. Singh K, Marchand B, Kirby KA, Michailidis E, Sarafianos SG (2010) Structural aspects of drug resistance and inhibition of HIV-1 reverse transcriptase. Viruses 2: 606–638.
5. Mas A, Parera M, Briones C, Soriano V, Martinez MA, et al. (2000) Role of a dipeptide insertion between codons 69 and 70 of HIV-1 reverse transcriptase in the mechanism of AZT resistance. EMBO J 19: 5752–5761.
6. Matamoros T, Franco S, Vazquez-Alvarez BM, Mas A, Martinez MA, et al. (2004) Molecular determinants of multi-nucleoside analogue resistance in HIV-1 reverse transcriptases containing a dipeptide insertion in the fingers subdomain: effect of mutations D67N and T215Y on removal of thymidine nucleotide analogues from blocked DNA primers. J Biol Chem 279: 24569–24577.
7. Meyer PR, Lennerstrand J, Matsuura SE, Larder BA, Scott WA (2003) Effects of dipeptide insertions between codons 69 and 70 of human immunodeficiency virus type 1 reverse transcriptase on primer unblocking, deoxynucleoside triphosphate inhibition, and DNA chain elongation. J Virol 77: 3871–3877.
8. Kew Y, Olsen LR, Japour AJ, Prasad VR (1998) Insertions into the beta3-beta4 hairpin loop of HIV-1 reverse transcriptase reveal a role for fingers subdomain in processive polymerization. J Biol Chem 273: 7529–7537.
9. Boyer PL, Sarafianos SG, Arnold E, Hughes SH (2002) Nucleoside analog resistance caused by insertions in the fingers of human immunodeficiency virus type 1 reverse transcriptase involves ATP-mediated excision. J Virol 76: 9143–9151.
10. Menendez-Arias L (2008) Mechanisms of resistance to nucleoside analogue inhibitors of HIV-1 reverse transcriptase. Virus Res 134: 124–146.
11. Sarafianos SG, Marchand B, Das K, Himmel DM, Parniak MA, et al. (2009) Structure and function of HIV-1 reverse transcriptase: molecular mechanisms of polymerization and inhibition. J Mol Biol 385: 693–713.
12. Sarafianos SG, Das K, Clark AD, Jr., Ding J, Boyer PL, et al. (1999) Lamivudine (3TC) resistance in HIV-1 reverse transcriptase involves steric hindrance with beta-branched amino acids. Proc Natl Acad Sci U S A 96: 10027–10032.
13. Gao HQ, Boyer PL, Sarafianos SG, Arnold E, Hughes SH (2000) The role of steric hindrance in 3TC resistance of human immunodeficiency virus type-1 reverse transcriptase. J Mol Biol 300: 403–418.

14. Shafer RW, Kozal MJ, Winters MA, Iversen AK, Katzenstein DA, et al. (1994) Combination therapy with zidovudine and didanosine selects for drug-resistant human immunodeficiency virus type 1 strains with unique patterns of pol gene mutations. J Infect Dis 169: 722–729.
15. Shirasaka T, Kavlick MF, Ueno T, Gao WY, Kojima E, et al. (1995) Emergence of human immunodeficiency virus type 1 variants with resistance to multiple dideoxynucleosides in patients receiving therapy with dideoxynucleosides. Proc Natl Acad Sci U S A 92: 2398–2402.
16. Iversen AK, Shafer RW, Wehrly K, Winters MA, Mullins JI, et al. (1996) Multidrug-resistant human immunodeficiency virus type 1 strains resulting from combination antiretroviral therapy. J Virol 70: 1086–1090.
17. Maeda Y, Venzon DJ, Mitsuya H (1998) Altered drug sensitivity, fitness, and evolution of human immunodeficiency virus type 1 with pol gene mutations conferring multi-dideoxynucleoside resistance. J Infect Dis 177: 1207–1213.
18. Matsumi S, Kosalaraksa P, Tsang H, Kavlick MF, Harada S, et al. (2003) Pathways for the emergence of multi-dideoxynucleoside-resistant HIV-1 variants. AIDS 17: 1127–1137.
19. Kosalaraksa P, Kavlick MF, Maroun V, Le R, Mitsuya H (1999) Comparative fitness of multi-dideoxynucleoside-resistant human immunodeficiency virus type 1 (HIV-1) in an In vitro competitive HIV-1 replication assay. J Virol 73: 5356–5363.
20. Garcia Lerma J, Schinazi RF, Juodawlkis AS, Soriano V, Lin Y, et al. (1999) A rapid non-culture-based assay for clinical monitoring of phenotypic resistance of human immunodeficiency virus type 1 to lamivudine (3TC). Antimicrob Agents Chemother 43: 264–270.
21. Feng JY, Myrick F, Selmi B, Deval J, Canard B, et al. (2005) Effects of HIV Q151M-associated multi-drug resistance mutations on the activities of (-)-beta-D-1′,3′-dioxolan guanine. Antiviral Res 66: 153–158.
22. Miller MD, Margot NA, Hertogs K, Larder B, Miller V (2001) Antiviral activity of tenofovir (PMPA) against nucleoside-resistant clinical HIV samples. Nucleosides Nucleotides Nucleic Acids 20: 1025–1028.
23. Smith RA, Gottlieb GS, Anderson DJ, Pyrak CL, Preston BD (2008) Human immunodeficiency virus types 1 and 2 exhibit comparable sensitivities to Zidovudine and other nucleoside analog inhibitors in vitro. Antimicrob Agents Chemother 52: 329–332.
24. Ueno T, Shirasaka T, Mitsuya H (1995) Enzymatic characterization of human immunodeficiency virus type 1 reverse transcriptase resistant to multiple 2′,3′-dideoxynucleoside 5′-triphosphates. J Biol Chem 270: 23605–23611.
25. Deval J, Selmi B, Boretto J, Egloff MP, Guerreiro C, et al. (2002) The molecular mechanism of multidrug resistance by the Q151M human immunodeficiency virus type 1 reverse transcriptase and its suppression using alpha-boranophosphate nucleotide analogues. J Biol Chem 277: 42097–42104.
26. Huang H, Chopra R, Verdine GL, Harrison SC (1998) Structure of a covalently trapped catalytic complex of HIV-1 reverse transcriptase: implications for drug resistance. Science 282: 1669–1675.
27. Sarafianos SG, Das K, Hughes SH, Arnold E (2004) Taking aim at a moving target: designing drugs to inhibit drug-resistant HIV-1 reverse transcriptases. Curr Opin Struct Biol 14: 716–730.
28. Gu Z, Fletcher RS, Arts EJ, Wainberg MA, Parniak MA (1994) The K65R mutant reverse transcriptase of HIV-1 cross-resistant to 2′, 3′-dideoxycytidine, 2′,3′-dideoxy-3′-thiacytidine, and 2′,3′-dideoxyinosine shows reduced sensitivity to specific dideoxynucleoside triphosphate inhibitors in vitro. J Biol Chem 269: 28118–28122.
29. Winters MA, Shafer RW, Jellinger RA, Mamtora G, Gingeras T, et al. (1997) Human immunodeficiency virus type 1 reverse transcriptase genotype and drug susceptibility changes in infected individuals receiving dideoxyinosine monotherapy for 1 to 2 years. Antimicrob Agents Chemother 41: 757–762.
30. Harrigan PR, Stone C, Griffin P, Najera I, Bloor S, et al. (2000) Resistance profile of the human immunodeficiency virus type 1 reverse transcriptase inhibitor abacavir (1592U89) after monotherapy and combination therapy. CNA2001 Investigative Group. J Infect Dis 181: 912–920.
31. Margot NA, Isaacson E, McGowan I, Cheng AK, Schooley RT, et al. (2002) Genotypic and phenotypic analyses of HIV-1 in antiretroviral-experienced patients treated with tenofovir DF. AIDS 16: 1227–1235.
32. Sluis-Cremer N, Arion D, Kaushik N, Lim H, Parniak MA (2000) Mutational analysis of Lys65 of HIV-1 reverse transcriptase. Biochem J 348 Pt 1: 77–82.
33. Deval J, Navarro JM, Selmi B, Courcambeck J, Boretto J, et al. (2004) A loss of viral replicative capacity correlates with altered DNA polymerization kinetics by the human immunodeficiency virus reverse transcriptase bearing the K65R and L74V dideoxynucleoside resistance substitutions. J Biol Chem 279: 25489–25496.
34. Feng JY, Myrick FT, Margot NA, Mulamba GB, Rimsky L, et al. (2006) Virologic and enzymatic studies revealing the mechanism of K65R- and Q151M-associated HIV-1 drug resistance towards emtricitabine and lamivudine. Nucleosides Nucleotides Nucleic Acids 25: 89–107.
35. Das K, Bandwar RP, White KL, Feng JY, Sarafianos SG, et al. (2009) Structural basis for the role of the K65r mutation in HIV-1 reverse transcriptase polymerization, excision antagonism, and tenofovir resistance. J Biol Chem 284: 35092–35100.
36. McColl DJ, Miller MD (2003) The use of tenofovir disoproxil fumarate for the treatment of nucleoside-resistant HIV-1. J Antimicrob Chemother 51: 219–223.
37. Chappell BJ, Margot NA, Miller MD (2007) Long-term follow-up of patients taking tenofovir DF with low-level HIV-1 viremia and the K65R substitution in HIV-1 RT. AIDS 21: 761–763.
38. Hachiya A, Kodama EN, Sarafianos SG, Schuckmann MM, Sakagami Y, et al. (2008) Amino acid mutation N348I in the connection subdomain of human immunodeficiency virus type 1 reverse transcriptase confers multiclass resistance to nucleoside and nonnucleoside reverse transcriptase inhibitors. J Virol 82: 3261–3270.
39. Shimura K, Kodama E, Sakagami Y, Matsuzaki Y, Watanabe W, et al. (2008) Broad antiretroviral activity and resistance profile of the novel human immunodeficiency virus integrase inhibitor elvitegravir (JTK-303/GS-9137). J Virol 82: 764–774.
40. Hachiya A, Aizawa-Matsuoka S, Tanaka M, Takahashi Y, Ida S, et al. (2001) Rapid and simple phenotypic assay for drug susceptibility of human immunodeficiency virus type 1 using CCR5-expressing HeLa/CD4(+) cell clone 1-10 (MAGIC-5). Antimicrob Agents Chemother 45: 495–501.
41. Michailidis E, Marchand B, Kodama EN, Singh K, Matsuoka M, et al. (2009) Mechanism of inhibition of HIV-1 reverse transcriptase by 4′-Ethynyl-2-fluoro-2′-deoxyadenosine triphosphate, a translocation-defective reverse transcriptase inhibitor. J Biol Chem 284: 35681–35691.
42. Singh K, Srivastava A, Patel SS, Modak MJ (2007) Participation of the fingers subdomain of Escherichia coli DNA polymerase I in the strand displacement synthesis of DNA. J Biol Chem 282: 10594–10604.
43. Kati WM, Johnson KA, Jerva LF, Anderson KS (1992) Mechanism and fidelity of HIV reverse transcriptase. J Biol Chem 267: 25988–25997.
44. Schuckmann MM, Marchand B, Hachiya A, Kodama EN, Kirby KA, et al. The N348I mutation at the connection subdomain of HIV-1 reverse transcriptase decreases binding to nevirapine. J Biol Chem.
45. Tuske S, Sarafianos SG, Clark AD, Jr., Ding J, Naeger LK, et al. (2004) Structures of HIV-1 RT-DNA complexes before and after incorporation of the anti-AIDS drug tenofovir. Nat Struct Mol Biol 11: 469–474.
46. Ren J, Nichols CE, Chamberlain PP, Weaver KL, Short SA, et al. (2004) Crystal structures of HIV-1 reverse transcriptases mutated at codons 100, 106 and 108 and mechanisms of resistance to non-nucleoside inhibitors. J Mol Biol 336: 569–578.
47. Clark S, Calef C, J M (2006) Mutations in Retroviral Genes Associated with Drug Resistance. HIV Sequence Compendium 2005: 58–175.
48. Meyer PR, Matsuura SE, So AG, Scott WA (1998) Unblocking of chain-terminated primer by HIV-1 reverse transcriptase through a nucleotide-dependent mechanism. Proc Natl Acad Sci U S A 95: 13471–13476.
49. Rigourd M, Ehresmann C, Parniak MA, Ehresmann B, Marquet R (2002) Primer unblocking and rescue of DNA synthesis by azidothymidine (AZT)-resistant HIV-1 reverse transcriptase: comparison between initiation and elongation of reverse transcription and between (−) and (+) strand DNA synthesis. J Biol Chem 277: 18611–18618.
50. Frankel FA, Marchand B, Turner D, Gotte M, Wainberg MA (2005) Impaired rescue of chain-terminated DNA synthesis associated with the L74V mutation in human immunodeficiency virus type 1 reverse transcriptase. Antimicrob Agents Chemother 49: 2657–2664.
51. Winters B, Montaner J, Harrigan PR, Gazzard B, Pozniak A, et al. (2008) Determination of clinically relevant cutoffs for HIV-1 phenotypic resistance estimates through a combined analysis of clinical trial and cohort data. J Acquir Immune Defic Syndr 48: 26–34.
52. Van Houtte M, Picchio G, Van Der Borght K, Pattery T, Lecocq P, et al. (2009) A comparison of HIV-1 drug susceptibility as provided by conventional phenotyping and by a phenotype prediction tool based on viral genotype. J Med Virol 81: 1702–1709.
53. Delaugerre C, Flandre P, Marcelin AG, Descamps D, Tamalet C, et al. (2008) National survey of the prevalence and conditions of selection of HIV-1 reverse transcriptase K70E mutation. J Med Virol 80: 762–765.
54. Kagan RM, Lee TS, Ross L, Lloyd RM, Jr., Lewinski MA, et al. (2007) Molecular basis of antagonism between K70E and K65R tenofovir-associated mutations in HIV-1 reverse transcriptase. Antiviral Res 75: 210–218.
55. Sluis-Cremer N, Sheen CW, Zelina S, Torres PS, Parikh UM, et al. (2007) Molecular mechanism by which the K70E mutation in human immunodeficiency virus type 1 reverse transcriptase confers resistance to nucleoside reverse transcriptase inhibitors. Antimicrob Agents Chemother 51: 48–53.
56. Van Laethem K, Pannecouque C, Vandamme AM (2007) Mutations at 65 and 70 within the context of a Q151M cluster in human immunodeficiency virus type 1 reverse transcriptase impact the susceptibility to the different nucleoside reverse transcriptase inhibitors in distinct ways. Infect Genet Evol 7: 600–603.
57. Larder BA, Kemp SD (1989) Multiple mutations in HIV-1 reverse transcriptase confer high-level resistance to zidovudine (AZT). Science 246: 1155–1158.
58. Johnson VA, Brun-Vezinet F, Clotet B, Gunthard HF, Kuritzkes DR, et al. (2009) Update of the drug resistance mutations in HIV-1: December 2009. Top HIV Med 17: 138–145.
59. Frangeul A, Bussetta C, Deval J, Barral K, Alvarez K, et al. (2008) Gln151 of HIV-1 reverse transcriptase acts as a steric gate towards clinically relevant acyclic phosphonate nucleotide analogues. Antivir Ther 13: 115–124.
60. Garforth SJ, Kim TW, Parniak MA, Kool ET, Prasad VR (2007) Site-directed mutagenesis in the fingers subdomain of HIV-1 reverse transcriptase reveals a specific role for the beta3-beta4 hairpin loop in dNTP selection. J Mol Biol 365: 38–49.
61. Sarafianos SG, Pandey VN, Kaushik N, Modak MJ (1995) Glutamine 151 participates in the substrate dNTP binding function of HIV-1 reverse transcriptase. Biochemistry 34: 7207–7216.

62. Frangeul A, Barral K, Alvarez K, Canard B (2007) In vitro suppression of K65R reverse transcriptase-mediated tenofovir- and adefovir-5′-diphosphate resistance conferred by the boranophosphonate derivatives. Antimicrob Agents Chemother 51: 3162–3167.
63. Sarafianos SG, Pandey VN, Kaushik N, Modak MJ (1995) Site-directed mutagenesis of arginine 72 of HIV-1 reverse transcriptase. Catalytic role and inhibitor sensitivity. J Biol Chem 270: 19729–19735.
64. Tu X, Das K, Han Q, Bauman JD, Clark AD, Jr., et al. Structural basis of HIV-1 resistance to AZT by excision. Nat Struct Mol Biol 17: 1202–1209.

Cell. Mol. Biol. 57 (1): 39-
Published on January 31, 2011; DOI 10.1170/T900

THE SUGAR RING CONFORMATION OF 4'-ETHYNYL-2-FLUORO-2'-DEOXYADENOSINE AND ITS RECOGNITION BY THE POLYMERASE ACTIVE SITE OF HIV REVERSE TRANSCRIPTASE

K.A. KIRBY[1], K. SINGH[1], E. MICHAILIDIS[1], B. MARCHAND[1], E.N. KODAMA[2], N. ASHIDA[3], H. MITSUYA[4], M.A. PARNIAK[5], AND S.G. SARAFIANOS[1]✉

1 Christopher S. Bond Life Sciences Center, Department of Molecular Microbiology & Immunology, University of Missouri School of Medicine, Columbia, MO 65211, USA
2 Division of Emerging Infectious Diseases. Tohoku University School of Medicine, Sendai 980-8575, Japan
3 Yamasa Corporation, Chiba 288-0056, Japan
4 Department of Hematology and Infectious Diseases, Kumamoto University, Kumamoto 860-8556, Japan & Experimental Retrovirology Section, HIV/AIDS Malignancy Branch, NIH, Bethesda, MD 20892, USA
5 Department of Molecular Genetics & Biochemistry University of Pittsburgh School of Medicine, Pittsburgh, PA 15261, USA

Abstract

4'-Ethynyl-2-fluoro-2'-deoxyadenosine (EFdA) is the most potent inhibitor of HIV reverse transcriptase (RT). We have recently named EFdA a Translocation Defective RT Inhibitor (TDRTI) because after its incorporation in the nucleic acid it blocks DNA polymerization, primarily by preventing translocation of RT on the template/primer that has EFdA at the 3'-primer end (T/P_{EFdA}). The sugar ring conformation of EFdA may also influence RT inhibition by a) affecting the binding of EFdA triphosphate (EFdATP) at the RT active site and/or b) by preventing proper positioning of the 3'-OH of EFdA in T/P_{EFdA} that is required for efficient DNA synthesis. Specifically, the North (C2'-exo/C3'-endo), but not the South (C2'-endo/C3'-exo) nucleotide sugar ring conformation is required for efficient binding at the primer-binding and polymerase active sites of RT. In this study we use nuclear magnetic resonance (NMR) spectroscopy experiments to determine the sugar ring conformation of EFdA. We find that unlike adenosine nucleosides unsubstituted at the 4'-position, the sugar ring of EFdA is primarily in the North conformation. This difference in sugar ring puckering likely contributes to the more efficient incorporation of EFdATP by RT than dATP. In addition, it suggests that the 3'-OH of EFdA in T/P_{EFdA} is not likely to prevent incorporation of additional nucleotides and thus it does not contribute to the mechanism of RT inhibition. This study provides the first insights into how structural attributes of EFdA affect its antiviral potency through interactions with its RT target.

Key words: EFdA, Translocation Defective Reverse Transcriptase Inhibitors, Sugar Ring Conformation, Reverse Transcriptase, HIV, Antivirals.

Article information's
Received on December 17, 2010
Accepted on January 5, 2011

Corresponding author
Stefan G. Sarafianos, Ph.D.
471d Christopher S. Bond Life Sciences Center,
1201 Rollins St., Columbia, MO 65211, USA
Fax: +1 (573) 884 - 9676
E-mail: sarafianoss@missouri.edu

Abbreviations: **dA** : 2'-Deoxyadenosine ; **dATP** : 2'-Deoxyadenosine triphosphate ; **EFdA** : 4'-Ethynyl-2-fluoro-2'-deoxyadenosine ; **EFdAMP** : 4'-Ethynyl-2-fluoro-2'-deoxyadenosine monophosphate ; **EFdATP** : 4'-Ethynyl-2-fluoro-2'-deoxyadenosine triphosphate; **NRTI** : Nucleoside reverse transcriptase inhibitor; **RT** : Reverse transcriptase; **T/P_{EFdA}** : Template/Primer terminated 4'-ethynyl-2-fluoro-2'-deoxyadenosine; **TDRTI**: Translocation defective reverse transcriptase inhibitor.

INTRODUCTION

HIV-1 reverse transcriptase (RT) is the most targeted viral protein by approved anti-HIV drugs due to its critical role in replication of the virus (24, 14, 29, 5, 32, 8). These inhibitors, which are either nucleoside reverse transcriptase inhibitors (NRTIs) or non-nucleoside reverse transcriptase inhibitors (NNRTIs), interfere with the enzyme's ability to synthesize the viral DNA. In particular, NRTIs mimic the natural dNTP substrate of the enzyme and bind to the 3'-primer terminus in the polymerase active site. Once incorporated into the primer, the NRTI prevents further elongation of the DNA by acting as a chain terminator. All currently approved NRTIs lack a 3'-OH moiety,

which has long been considered a requirement for inhibitors to be successful chain terminators. Although this lack of a 3'-OH group promotes effective chain termination, it imparts a negative effect on the potency of the NRTI, including a diminished binding affinity for the RT target and decreased ability to be activated by cellular kinases (12).

We reported previously that a group of NRTIs with 4'-substitutions and a 3'-OH are very effective at inhibiting both wild-type (WT) and multi-drug resistant strains of HIV (18). The most potent compound in this collection is 4'-ethynyl-2-fluoro-2'-deoxyadenosine (EFdA), an adenosine analog containing a 4'-ethynyl group on the deoxyribose ring and a 2-fluoro group on the adenine base (Figure 1). EFdA is able to inhibit both WT and multi-drug resistant strains of HIV several orders of magnitude more efficiently than all other currently approved NRTIs (22). Moreover, clinically-observed drug resistant HIV strains are sensitive (38, 21), and in some cases hypersensitive (17), to EFdA. Recently, we have shown that EFdA acts primarily as a chain terminator because it prevents translocation of RT on the EFdA-terminated primer after incorporation. Antiviral compounds demonstrating this novel mechanism of inhibition have been termed Translocation Defective Reverse Transcriptase Inhibitors (TDRTIs) (22).

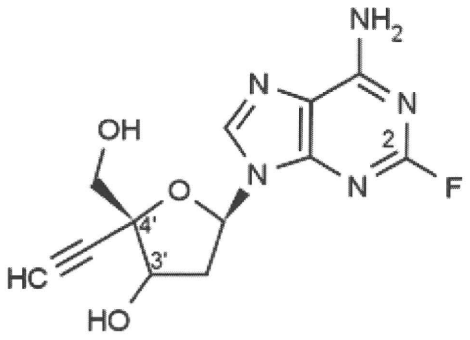

Figure 1. The chemical structure of EFdA.

It has been demonstrated that the conformation of the sugar ring affects the biological activity of NRTIs (16, 30, 27, 20, 25, 4, 31, 2, 3). In solution, the structure of the deoxyribose ring of nucleosides exists in a dynamic equilibrium between the C2'-exo/C3'-endo (North) and C2'-endo/C3'-exo (South) conformations. It has previously been shown that the sugar ring conformation of NRTIs is important for recognition by RT at both the primer and dNTP binding sites. For efficient DNA polymerization to occur, both the nucleotide at the 3'-end of the primer and the incoming dNTP or NRTI are required to be in the North conformation. In the North conformation, the 3'-OH of the nucleotide at the 3'-primer terminus is properly positioned for in-line nucleophilic attack on the α-phosphate of the incoming dNTP or NRTI (Figure 2a). The North conformation is also important for the incoming dNTP or NRTI, because if the sugar ring were in the South conformation, the 3'-OH would be very close to Tyr115 of RT (d = 1.8 Å), creating unfavorable steric interactions between the substrate and enzyme (Figure 2b) (20, 23, 2).

If EFdA were in the South conformation after incorporation into the primer, then the 3'-OH would not be properly positioned for in-line nucleophilic attack on the α-phosphate of the next incoming nucleotide, therefore contributing to inefficient catalysis and inhibition of DNA synthesis. In order to evaluate the influence of these structural attributes on the antiviral properties of EFdA, we carried out nuclear magnetic resonance (NMR) spectroscopy experiments using EFdA and the natural substrate dA. The results of this study allow us to compare the sugar ring puckering of EFdA and other nucleoside analogs, such as 2'-fluoro-2',3'-dideoxynucleoside 5'-triphosphates (23), AZT, ddI, ddA (26), and bicyclo[3.1.0]hexene nucleosides (28), and determine if its structure 1) is in the proper conformation for optimal recognition by RT and 2) if it contributes to the inhibition mechanism of HIV RT.

MATERIALS AND METHOD

Chemicals

The compound dA was purchased from Sigma-Aldrich (St. Louis, MO). EFdA was provided by Yamasa Corporation (Chiba, Japan). d_6-Dimethyl sulfoxide (DMSO) was purchased from Cambridge Isotope Laboratories, Inc. (Andover, MA). All other materials were purchased from Fisher Scientific (Pittsburgh, PA).

NMR Spectroscopy

One-dimensional ^{1}H NMR spectra were collected in 10 °C increments from 20 to 50 °C on a Bruker Avance DRX500 Spectrometer equipped with a 5mm HCN cryoprobe. Both dA and EFdA were dissolved in d_6-DMSO to final concentrations of 2 – 4 mM. Spectra used for coupling constant analysis were acquired with 64 scans and 33K data points with a sweep width of 4960 Hz and a relaxation delay of 4.3 s. Spectra were processed with a line broadening of 0.3 Hz. Coupling constants were read

directly from the spectra for first-order resonances. Complex multiplets were analyzed by spectral simulation using SpinWorks 3.0 (19). Simulations were performed for the spin systems on the deoxyribose ring only. RMS deviations of calculated and experimental coupling constants for both compounds were < 0.05 Hz.

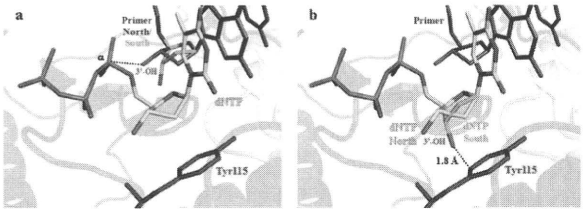

Figure 2. The effect of sugar ring conformation in the HIV-1 RT polymerase active site. The sugar ring conformation at the 3'-primer end is required to be in the North (2'-exo/3'-endo) conformation (2a, dark gray) for successful in-line nucleophilic attack of the α-phosphate of the incoming dNTP or NRTI. The South (2'-endo/3'-exo) (2a, green) conformation of the sugar ring at the primer terminus positions the 3'-OH away from the α-phosphate and thus DNA polymerization is not as efficient. The preferred conformation of the sugar ring of the incoming dNTP or NRTI is the North conformation (2b, yellow). The South conformation of the sugar ring of the incoming dNTP or NRTI (2b, green) would result in a very short distance between the 3'-OH and the aromatic ring of Tyr115 (red), causing steric interactions with the enzyme. Coot (10) was used to perform simple modeling of the 2'-endo/3'-exo sugar ring conformations of the primer and dNTP using structural coordinates from PDB Code 1RTD. Images were generated using PyMOL (7).

Pseudorotational Analysis

Sugar ring conformations of dA and EFdA were determined using the program PSEUROT 6.3 (13, 6, 36) (acquired from Dr. Cornelis Altona, University of Leiden, Netherlands). This version utilizes an improved generalized Karplus equation, as described by Donders et al. (9), which uses experimental data as a basis for the iterative calculation of coupling constants. In the case of dA, the puckering amplitude of the less favored conformation ($\phi_m(N)$) was held constant during calculations. For EFdA, the puckering amplitudes of both conformations were fixed during calculation. RMS deviations of calculated and experimental coupling constants for both compounds were < 0.2 Hz.

Molecular Modeling

A model of the ternary complex of HIV-1 RT / DNA / EFdA triphosphate (EFdATP) was built using the coordinates of the crystal structure of the HIV-1 RT-DNA-tenofovir diphosphate (TFVDP) complex (35). The triphosphate of the EFdATP was built using the corresponding atoms of TFVDP in the structure from PDB code 1T05 and of dTTP in PDB code 1RTD (15). The structure of the EFdATP was assembled from its components using the sketch module of SYBYL 7.3 (34), and minimized by the semi-empirical quantum chemical method PM3 (33). After removing the TFVDP from 1T05, the PM3 charges and the docking module of SYBYL 7.0 were used to dock the EFdATP at the RT dNTP binding site to give the ternary complex of HIV-1 RT / DNA / EFdATP. The final complex structure was minimized for 100 cycles using the AMBER force field with Coleman united charges on the protein and DNA molecules.

RESULTS

NMR Spectroscopy and Pseudorotational Analysis

To evaluate the sugar ring conformation of dA and EFdA, one-dimensional ^{1}H NMR spectra were collected over a range of temperatures for both compounds. Coupling constants determined from each spectrum were used to calculate the structural parameters of the deoxyribose ring. The changes in the value of each coupling constant with temperature were examined for both compounds, and these changes were used to calculate the pseudorotational phase angle, P, and the degree of maximum ring pucker, ϕ_m, using PSEUROT 6.3 (Table 1) (1).

Coupling constants between most of the hydrogen atoms on the deoxyribose ring required spectral simulation in order to be resolved. The pseudorotational parameters listed in Table 1 were calculated with PSEUROT 6.3, which assumes a two-state approximation (North and South) and utilizes a generalized Karplus equation combined with a non-linear Newton-Raphson minimization process to examine the conformational flexibility of five-membered rings. An iterative approach was used to determine the optimal pseudorotational parameters P_N, P_S, $\phi_m(N)$, and $\phi_m(S)$ in which some of these parameters were fixed during refinement.

The results of the conformational analysis of dA demonstrate that the sugar ring heavily favors the South conformation over the North conformation in solution. This result is in agreement with previous conformational studies of dA (37, 11). On the other hand, the results of the conformational analysis of EFdA show that the sugar ring favors the North conformation in solution (Figure 3). The value of P_N is 38.7°, which is just slightly outside of the range observed for most typical nucleosides (P_N = 0 – 36°) but still in the Northern hemisphere (1). This observation is similar to that previously reported for 4'-ethynyl-2',3'-dideoxycytidine (31). The value of P_S is 146.5°, which falls in the range commonly observed for traditional nucleosides (P_S = 144 – 180°). The values of

Table 1. Summary of pseudorotational analysis. [a]Root mean square deviation between experimental and calculated coupling constants. [b]Parameter fixed during calculations.

Compound	P_N, deg	P_S, deg	$\phi_m(N)$, deg	$\phi_m(S)$, deg	% N	RMS error (Hz)[a]
dA	18.7	169.1	39.0[b]	31.1	23	0.034
EFdA	38.7	146.5	39.0[b]	39.0[b]	75	0.197

$\phi_m(N)$ and $\phi_m(S)$ were fixed during calculations to 39°, the average value commonly observed for purine-base nucleosides (1). This result suggests that either the 4'-ethynyl, 2-fluoro, or both in combination greatly influence the sugar ring conformation of EFdA compared to the natural substrate, dA.

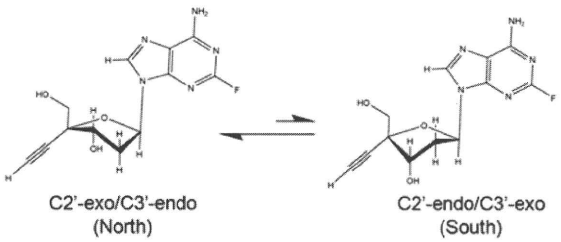

Figure 3. Dynamic equilibrium between the North and South sugar ring conformations of EFdA in solution.

To understand the molecular basis of importance of the sugar ring conformation for RT recognition, we used our pre-catalytic RT / DNA / EFdATP ternary complex to assess the effect of EFdA sugar ring conformation on the binding interactions of the inhibitor with the polymerase active site of the enzyme (Figure 4). In our molecular model, the 4'-ethynyl group is stabilized in a hydrophobic pocket formed by RT residues Ala114, Tyr115, Phe160, Met184, and the aliphatic segment of Asp185. With the 3'-carbon in the North conformation, the 3'-OH is able to fit nicely in the RT polymerase active site. However, when the 3'-carbon of EFdATP is placed in the South conformation, the 3'-OH interacts sterically with the aromatic ring of Tyr115 (short distance of 1.8 Å).

DISCUSSION

Our results show that EFdA has a dramatically different sugar ring conformation than dA. The equilibrium between the North and South sugar ring conformations is shifted from the preferred South conformation for the natural substrate dA to the North conformation for EFdA. It is not clear if the structural changes are due to the 2- or 4'-substitutions in EFdA. However, it is likely that steric interactions between the 4'-ethynyl and the 3'-OH disfavor the South conformation of EFdA. This is because the North conformation of the sugar ring positions the 4'-ethynyl and the 3'-OH groups farther apart than they would be in the South conformation. However, even in the absence of the 3'-OH, the sugar ring in the crystal structure of 4'-ethynyl-2',3'-dideoxycytidine is also in the North conformation (31). Hence, it appears that in addition to steric interactions between the 3'-OH and 4'-ethynyl, other factors contribute to the propensity of 4'-ethynyl-substituted NRTIs to have a sugar ring in the North conformation.

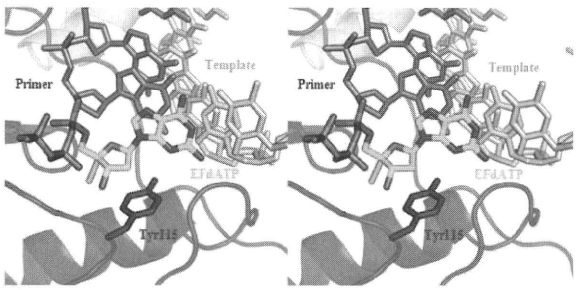

Figure 4. Stereo view of EFdATP (cyan) modeled in the RT active site. The 3'-OH of EFdATP is in the North conformation and is free of steric interactions with Tyr115 (red sticks). The primer is in dark gray, the template in light gray, the connection subdomain in yellow, and the palm subdomain in red. The fingers subdomain was removed for clarity. Image generated using PyMOL (7).

The NMR experiments confirm that EFdA is primarily in the North conformation, rendering its structure (and presumably the structure of its active metabolite EFdATP) in the optimal conformation for binding at the polymerase active site of RT. While the natural substrate, dA, favors the South conformation, the energy barrier required to convert the sugar ring of dA to the North conformation is very small, approximately 1 kcal/mol (11). EFdA (and presumably EFdATP) already favors the North conformation and does not have to overcome this energy barrier in order to bind to the primer. This is likely a contributing factor in the more

efficient incorporation of EFdATP into the primer strand than dATP, contributing to the high potency of the inhibitor as reported (22).

Molecular modeling studies were performed with EFdATP to gain further insight into the structural effects of the sugar ring conformation on RT recognition. When EFdATP is positioned in the nucleotide binding site prior to incorporation into the primer, the importance of the sugar ring puckering becomes apparent. With the sugar ring of EFdATP positioned in the North conformation, the 3'-OH is free of unfavorable interactions with RT (particularly from steric interactions with Tyr115) and fits perfectly in the active site. In addition, the sugar ring geometry of EFdA allows favorable interactions of the 4'-ethynyl into a hydrophobic pocket defined by RT residues A114, Y115, F160, M184 and the aliphatic chain of D185. These interactions are thought to contribute both to enhanced RT utilization of EFdATP and difficulty in translocation of 3'-terminal EFdAMP primers (22).

Upon incorporation into the primer strand, the position of the 3'-OH of the EFdAMP in the North conformation is in perfect alignment for in-line nucleophilic attack on the α-phosphate of the next incoming dNTP. Because the North conformation of the sugar ring is heavily favored over the South conformation for EFdA, this is evidence that misalignment of the 3'-OH for nucleophilic attack is not a contributing factor to the chain termination mechanism of inhibition of EFdA. While the sugar ring conformation of the 3'-terminal EFdAMP is in the North conformation, which favors incorporation of the next dNTP, this step cannot occur because of the inability of RT to translocate from the nucleotide binding site. This further supports the observation that the inability of RT to translocate after EFdA incorporation is the primary mechanism of inhibition (22).

Slight changes in the chemical composition of adenosine analogs have a pronounced effect on the efficiency of TDRTIs in blocking HIV replication. In particular, substitutions at the 4'-position of the deoxyribose ring and the 2-position of the adenine base favor structural conformations of EFdA that improve its interactions with the RT target, thereby enhancing its antiviral potency.

Acknowledgements – We would like to thank Dr. Wei Wycoff for assistance with variable temperature NMR data collection. The purchase of the 500 MHz NMR spectrometer was partially supported by NSF grant CHE-89-08304, and NIH/NCRR grant S10 RR022341-01 (cold probe). This work was supported in part by NIH grants AI074389, AI076119, AI076119-S1, AI076119-02S1, and AI094715 (to S.G.S.) and AI079801 (to M.A.P.). We also acknowledge support from GeneMatrix and the Korea Food & Drug Administration and the Ministry of Knowledge and Economy, Bilateral International Collaborative R&D Program. B.M. is a recipient of the amfAR Mathilde Krim Fellowship. We are grateful to Yamasa Corporation for providing EFdA.

REFERENCES

1. Altona, C. and Sundaralingam, M., Conformational analysis of the sugar ring in nucleosides and nucleotides: A new description using the concept of pseudorotation. *J. Am. Chem. Soc.* 1972, **94**: 8205-8212.

2. Boyer, P.L., Julias, J.G., Marquez, V.E. and Hughes, S.H., Fixed conformation nucleoside analogs effectively inhibit excision-proficient HIV-1 reverse transcriptases. *J. Mol. Biol.* 2005, **345**: 441-450.

3. Boyer, P.L., Julias, J.G., Ambrose, Z., Siddiqui, M.A., Marquez, V.E. and Hughes, S.H., The nucleoside analogs 4'C-methyl thymidine and 4'C-ethyl thymidine block DNA synthesis by wild-type HIV-1 RT and excision proficient NRTI resistant RT variants. *J. Mol. Biol.* 2007, **371**: 873-882.

4. Choi, Y., George, C., Comin, M.J., Barchi, J.J., Jr., Kim, H.S., Jacobson, K.A., Balzarini, J., Mitsuya, H., Boyer, P.L., Hughes, S.H. and Marquez, V.E., A conformationally locked analogue of the anti-HIV agent stavudine. An important correlation between pseudorotation and maximum amplitude. *J. Med. Chem.* 2003, **46**: 3292-3299.

5. De Clercq, E., Anti-HIV drugs. *Verh. K. Acad. Geneeskd. Belg.* 2007, **69**: 81-104.

6. De Leeuw, F.A.A.M. and Altona, C., Computer assisted pseudorotational analysis of 5-membered rings by means of $^3J_{HH}$ coupling constants: program PSEUROT. *J. Comp. Chem.* 1983, **4**: 428-437.

7. DeLano, W.L. *The PyMOL Molecular Graphics System*, DeLano Scientific: Palo Alto, CA, USA, 2002. http://www.pymol.org.

8. Deval, J., Antimicrobial strategies: inhibition of viral polymerases by 3'-hydroxyl nucleosides. *Drugs* 2009, **69**: 151-166.

9. Donders, L.A., De Leeuw, F.A.A.M. and Altona, C., Relationship between proton-proton NMR coupling constants and substituent electronegativities. IV. An extended Karplus equation accounting for interactions between subtituents and its application to coupling constant data calculated by the extended Hueckel method. *Magn. Reson. Chem.* 1989, **27**: 556-563.

10. Emsley, P. and Cowtan, K., Coot: model-building tools for molecular graphics. *Acta Crystallogr. D Biol. Crystallogr.* 2004, **60**: 2126-2132.

11. Ford, H., Jr., Dai, F., Mu, L., Siddiqui, M.A., Nicklaus, M.C., Anderson, L., Marquez, V.E. and Barchi, J.J., Jr., Adenosine deaminase prefers a distinct sugar ring conformation for binding and catalysis: kinetic and structural studies. *Biochemistry.* 2000, **39**: 2581-2592.

12. Gallois-Montbrun, S., Schneider, B., Chen, Y., Giacomoni-Fernandes, V., Mulard, L., Morera, S., Janin, J.,

Deville-Bonne, D. and Veron, M., Improving nucleoside diphosphate kinase for antiviral nucleotide analogs activation. *J. Biol. Chem.* 2002, **277**: 39953-39959.

13. Haasnoot, C.A.G., De Leeuw, F.A.A.M., De Leeuw, H.P.M. and Altona, C., The relationship between proton-proton NMR coupling constants and substituent electronegativities II-Conformational analysis of the sugar ring in nucleosides and nucleotides in solution using a generalized Karplus equation. *Org. Magn. Reson.* 1981, **15**: 43-52.

14. Hammer, S.M., Saag, M.S., Schechter, M., Montaner, J.S., Schooley, R.T., Jacobsen, D.M., Thompson, M.A., Carpenter, C.C., Fischl, M.A., Gazzard, B.G., Gatell, J.M., Hirsch, M.S., Katzenstein, D.A., Richman, D.D., Vella, S., Yeni, P.G. and Volberding, P.A., Treatment for adult HIV infection: 2006 recommendations of the International AIDS Society--USA panel. *Top HIV Med.* 2006, **14**: 827-843.

15. Huang, H., Chopra, R., Verdine, G.L. and Harrison, S.C., Structure of a covalently trapped catalytic complex of HIV-1 reverse transcriptase: implications for drug resistance. *Science* 1998, **282**: 1669-1675.

16. Jagannadh, B., Reddy, D.V. and Kunwar, A.C., 1H NMR study of the sugar pucker of 2',3'-dideoxynucleosides with anti-human immunodeficiency virus (HIV) activity. *Biochem. Biophys. Res. Commun.* 1991, **179**: 386-391.

17. Kawamoto, A., Kodama, E., Sarafianos, S.G., Sakagami, Y., Kohgo, S., Kitano, K., Ashida, N., Iwai, Y., Hayakawa, H., Nakata, H., Mitsuya, H., Arnold, E. and Matsuoka, M., 2'-deoxy-4'-C-ethynyl-2-halo-adenosines active against drug-resistant human immunodeficiency virus type 1 variants. *Int. J. Biochem. Cell Biol.* 2008, **40**: 2410-2420.

18. Kodama, E.I., Kohgo, S., Kitano, K., Machida, H., Gatanaga, H., Shigeta, S., Matsuoka, M., Ohrui, H. and Mitsuya, H., 4'-Ethynyl nucleoside analogs: potent inhibitors of multidrug-resistant human immunodeficiency virus variants in vitro. *Antimicrob. Agents Chemother.* 2001, **45**: 1539-1546.

19. Marat, K. SpinWorks 3.0, released April 11, 2008. University of Manitoba, Winnipeg, Manitoba, Canada. http://www.umanitoba.ca/chemistry/nmr/spinworks/index.html.

20. Marquez, V.E., Ezzitouni, A., Russ, P., Siddiqui, M.A., Ford, H., Jr., Feldman, R.J., Mitsuya, H., George, C. and Barchi, J.J., Jr., HIV-1 Reverse Transcriptase Can Discriminate Between Two Conformationally Locked Carbocyclic AZT Triphosphate Analogues. *J. Am. Chem. Soc.* 1998, **120**: 2780-2789.

21. Mascolini, M., Larder, B.A., Boucher, C.A., Richman, D.D. and Mellors, J.W., Broad advances in understanding HIV resistance to antiretrovirals: report on the XVII International HIV Drug Resistance Workshop. *Antivir. Ther.* 2008, **13**: 1097-1113.

22. Michailidis, E., Marchand, B., Kodama, E.N., Singh, K., Matsuoka, M., Kirby, K.A., Ryan, E.M., Sawani, A.M., Nagy, E., Ashida, N., Mitsuya, H., Parniak, M.A. and Sarafianos, S.G., Mechanism of inhibition of HIV-1 reverse transcriptase by 4'-ethynyl-2-fluoro-2'-deoxyadenosine triphosphate, a translocation defective reverse transcriptase inhibitor. *J. Biol. Chem.* 2009, **284**: 35681-35691.

23. Mu, L., Sarafianos, S.G., Nicklaus, M.C., Russ, P., Siddiqui, M.A., Ford, H., Jr., Mitsuya, H., Le, R., Kodama, E., Meier, C., Knispel, T., Anderson, L., Barchi, J.J., Jr. and Marquez, V.E., Interactions of conformationally biased north and south 2'-fluoro-2', 3'-dideoxynucleoside 5'-triphosphates with the active site of HIV-1 reverse transcriptase. *Biochemistry.* 2000, **39**: 11205-11215.

24. Parniak, M.A. and Sluis-Cremer, N., Inhibitors of HIV-1 reverse transcriptase. *Adv. Pharmacol.* 2000, **49**: 67-109.

25. Poznanski, J., Bretner, M., Kulikowski, T., Balzarini, J., Van Aerschot, A. and De Clercq, E., Synthesis, solution conformation and anti-HIV activity of novel 3'-substituted-2',3'-dideoxy-5-hydroxymethyluridines and their 4,5-substituted analogues. *Antivir. Chem. Chemother.* 2003, **14**: 127-138.

26. Reddy, D.V., Jagannadh, B. and Kunwar, A.C., NMR study of dideoxynucleotides with anti-human immunodeficiency virus (HIV) activity. *J. Biochem. Biophys. Methods.* 1996, **31**: 113-121.

27. Rodriguez, J.B., Marquez, V.E., Nicklaus, M.C., Mitsuya, H. and Barchi, J.J., Jr., Conformationally locked nucleoside analogues. Synthesis of dideoxycarbocyclic nucleoside analogues structurally related to neplanocin C. *J. Med. Chem.* 1994, **37**: 3389-3399.

28. Russ, P.L., Gonzalez-Moa, M.J., Vu, B.C., Sigano, D.M., Kelley, J.A., Lai, C.C., Deschamps, J.R., Hughes, S.H. and Marquez, V.E., North- and south-bicyclo[3.1.0]hexene nucleosides: the effect of ring planarity on anti-HIV activity. *ChemMedChem.* 2009, **4**: 1354-1363.

29. Schinazi, R.F., Hernandez-Santiago, B.I. and Hurwitz, S.J., Pharmacology of current and promising nucleosides for the treatment of human immunodeficiency viruses. *Antiviral Res.* 2006, **71**: 322-334.

30. Siddiqui, M.A., Driscoll, J.S., Marquez, V.E., Roth, J.S., Shirasaka, T., Mitsuya, H., Barchi, J.J., Jr. and Kelley, J.A., Chemistry and anti-HIV properties of 2'-fluoro-2',3'-dideoxyarabinofuranosylpyrimidines. *J. Med. Chem.* 1992, **35**: 2195-2201.

31. Siddiqui, M.A., Hughes, S.H., Boyer, P.L., Mitsuya, H., Van, Q.N., George, C., Sarafinanos, S.G. and Marquez, V.E., A 4'-C-ethynyl-2',3'-dideoxynucleoside analogue highlights the role of the 3'-OH in anti-HIV active 4'-C-ethynyl-2'-deoxy nucleosides. *J. Med. Chem.* 2004, **47**: 5041-5048.

32. Sluis-Cremer, N. and Tachedjian, G., Mechanisms of inhibition of HIV replication by non-nucleoside reverse transcriptase inhibitors. *Virus Res.* 2008, **134**: 147-156.

33. Stewart, J.J.P., Optimization of parameters for semiempirical methods I. Method. *J. Comput. Chem.* 1989, **10**: 209-220.

34. *SYBYL 7.3*, Tripos International: 1699 South Hanley Rd., St. Louis, Missouri, 63144, USA.

35. Tuske, S., Sarafianos, S.G., Clark, A.D., Jr., Ding, J., Naeger, L.K., White, K.L., Miller, M.D., Gibbs, C.S., Boyer, P.L., Clark, P., Wang, G., Gaffney, B.L., Jones, R.A., Jerina, D.M., Hughes, S.H. and Arnold, E., Structures of HIV-1 RT-DNA complexes before and after incorporation of the anti-AIDS drug tenofovir. *Nat. Struct. Mol. Biol.* 2004, **11**: 469-474.

36. Van Wijk, J., Huckriede, B.D., Ippel, J.H. and Altona, C., Furanose sugar conformations in DNA from NMR coupling constants. *Methods Enzymol.* 1992, **211**: 286-306.

37. Westhof, E., Plach, H., Cuno, I. and Ludemann, H.-D., Proton magnetic resonance studies of 2'-, 3'-, and 5'-deoxyadenosine conformations in solution. *Nucelic Acids Res.* 1977, **4**: 939-953.

38. White, K.L., Chen, J.M., Feng, J.Y., Margot, N.A., Ly, J.K., Ray, A.S., Macarthur, H.L., McDermott, M.J., Swaminathan, S. and Miller, M.D., The K65R reverse transcriptase mutation in HIV-1 reverses the excision phenotype of zidovudine resistance mutations. *Antivir. Ther.* 2006, **11**: 155-163.

Bioorganic & Medicinal Chemistry Letters 20 (2010) 5853–5858

Contents lists available at ScienceDirect

Bioorganic & Medicinal Chemistry Letters

journal homepage: www.elsevier.com/locate/bmcl

CD4 mimics targeting the HIV entry mechanism and their hybrid molecules with a CXCR4 antagonist

Tetsuo Narumi [a], Chihiro Ochiai [a], Kazuhisa Yoshimura [b], Shigeyoshi Harada [b], Tomohiro Tanaka [a], Wataru Nomura [a], Hiroshi Arai [a], Taro Ozaki [a], Nami Ohashi [a], Shuzo Matsushita [b], Hirokazu Tamamura [a,*]

[a] Institute of Biomaterials and Bioengineering, Tokyo Medical and Dental University, Chiyoda-ku, Tokyo 101-0062, Japan
[b] Center for AIDS Research, Kumamoto University, Kumamoto 860-0811, Japan

ARTICLE INFO

Article history:
Received 14 June 2010
Revised 22 July 2010
Accepted 26 July 2010
Available online 3 August 2010

Keywords:
CD4
HIV entry
Hybrid molecule
gp120

ABSTRACT

Small molecules behaving as CD4 mimics were previously reported as HIV-1 entry inhibitors that block the gp120–CD4 interaction and induce a conformational change in gp120, exposing its co-receptor-binding site. A structure–activity relationship (SAR) study of a series of CD4 mimic analogs was conducted to investigate the contribution from the piperidine moiety of CD4 mimic **1** to anti-HIV activity, cytotoxicity, and CD4 mimicry effects on conformational changes of gp120. In addition, several hybrid molecules based on conjugation of a CD4 mimic analog with a selective CXCR4 antagonist were also synthesized and their utility evaluated.

The infection of host cells by HIV-1 takes place in multiple steps via a dynamic supramolecular mechanism mediated by two viral envelope glycoproteins (gp41, gp120) and several cell surface proteins (CD4, CCR5/CXCR4).[1] Cell penetration begins with the interaction of gp120 with the primary receptor CD4. This induces conformational changes in gp120, leading to the exposure of its V3 loop allowing the subsequent binding of gp120 to a co-receptor, CCR5[2] or CXCR4.[3]

N-(4-Chlorophenyl)-*N*′-(2,2,6,6-tetramethyl-piperidin-4-yl)oxalamide (NBD-556: **1**) and the related compounds NBD-557 (**2**) and YYA-021 (**3**) have been identified as a novel class of HIV-1 entry inhibitors, which exert potent cell fusion and virus cell fusion inhibitory activity at low micromolar levels (Fig. 1).[4] Furthermore, compound **1** can also induce thermodynamically favored conformational changes in gp120 similar to those caused by CD4 binding. The X-ray crystal structure of gp120 complexed with CD4 revealed the presence of a hydrophobic cavity, the Phe43 cavity, which is penetrated by the aromatic ring of Phe^{43} of CD4.[5] Molecular modeling revealed that compound **1** is also inserted into the Phe43 cavity, the *para*-chlorophenyl group of **1** entering more deeply than the phenyl ring of Phe^{43} of CD4 and interacting with the conserved gp120 residues such as Trp^{427}, Phe^{382}, and Trp^{112}.[4c] The modeling also suggested that an oxalamide linker forms hydrogen bonds with carbonyl groups of the gp120 backbone peptide bonds. Our model of **1** docked into gp120 revealed that eight other gp120 residues, Val^{255}, Asp^{368}, Glu^{370}, Ser^{375}, Ile^{424}, Trp^{427}, Val^{430}, and Val^{475} are located within a 4.4 Å-radius of **1** and that a large cavity exists around the *p*-position of the aromatic ring of **1**.[4e] Based on these observations, we conducted a structure–activity relationship (SAR) study of a series of analogs of CD4 mimics with substituents at the *p*-position of the aromatic ring. This study revealed that a certain size and electron-withdrawing ability of the substituents are indispensable for potent anti-HIV activity.[4e]

Although several reported SAR studies of **1** have revealed the contributions of the phenyl ring and the oxalamide linker of **1** to the binding affinity with gp120, the anti-HIV activity and the CD4 mimicry on conformational changes of gp120,[4] there has been, to the best of our knowledge, no prior report describing SAR studies of the piperidine ring of **1**. In this paper, the contributions of the piperidine ring of **1** to the anti-HIV activity, CD4 mimicry and cytotoxicity were investigated through the SAR studies focused on the piperidine ring of **1**. Furthermore, to apply the utility of CD4 mimics to the development of potent anti-HIV agents, a series of the

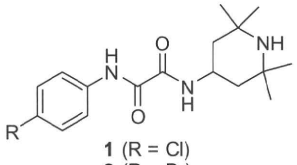

1 (R = Cl)
2 (R = Br)
3 (R = Me)

Figure 1. NBD-556 (**1**) and related compounds.

* Corresponding author.
E-mail address: tamamura.mr@tmd.ac.jp (H. Tamamura).

0960-894X/$ - see front matter © 2010 Elsevier Ltd. All rights reserved.
doi:10.1016/j.bmcl.2010.07.106

hybrid molecules that combined CD4 mimic analogs with a selective CXCR4 antagonist were also synthesized and bioevaluated.

For the design of novel CD4 mimic analogs, we initially tried to directly derivatize the nitrogen atom of piperidine group. However, direct alkylation and acylation of **1** failed probably as a result of steric hindrance from the methyl groups on the piperidine ring so we synthesized several derivatives lacking the methyl groups and evaluated their anti-HIV activity, cytotoxicity, and ability to mimic CD4. According to the previous SAR study,[4e] the *p*-Cl (**4**), *p*-Br (**5**) and *p*-methyl derivatives (**6**) lacking the methyl groups on the piperidine ring were prepared. Compounds **4–6** were synthesized by published methods as shown in Scheme 1. Briefly, coupling of aniline derivatives with ethyl chloroglyoxalate in the presence of Et_3N and subsequent saponification gave the corresponding acids (**10–12**). Condensation of these acids with 4-amino-*N*-benzylpiperidine in the presence of EDC–HOBt system, followed by debenzylation under von Braun conditions with 1-chloroethyl choroformate[6] produced the desired compounds **4–6**.[7]

The anti-HIV activity of each of the synthetic compounds was evaluated against MNA (R5) strain, with the results shown in Table 1. IC_{50} values were determined by the 3-(4,5-dimethylthiazol-2-yl)-2,5-diphenyltetrazolium bromide (MTT) method[8] as the concentrations of the compounds which conferred 50% protection against HIV-1-induced cytopathogenicity in PM1/CCR5 cells. Cytotoxicity of the compounds based on the viability of mock-infected PM1/CCR5 cells was also evaluated using the MTT method. CC_{50} values, the concentrations achieving 50% reduction of the viability of mock-infected cells, were also determined. Compounds **1** and **3** showed potent anti-HIV activity. The anti-HIV IC_{50} of compound **2** was previously reported to be comparable to that of compound **1**, and thus was not determined in this study. Novel derivatives **4** and **6** without the methyl groups on the piperidine ring, showed significant anti-HIV activity comparable to that of the parent compounds **1** and **3**, respectively. The *p*-methyl derivative **6** has slightly lower activity than the *p*-Cl derivative **4** and the *p*-Br derivative **5**. These results are consistent with our previous SAR studies on the parent compounds **1–3**. Compound **5** was found to exhibit relatively strong cytotoxicity (CC_{50} = 50 μM) and compounds **4** and **6** have cytotoxicities comparable to that of compounds **1** and **3**, respectively. This observation indicates that the methyl groups on the piperidine ring do not contribute significantly to the anti-HIV activity or the cytotoxicity.

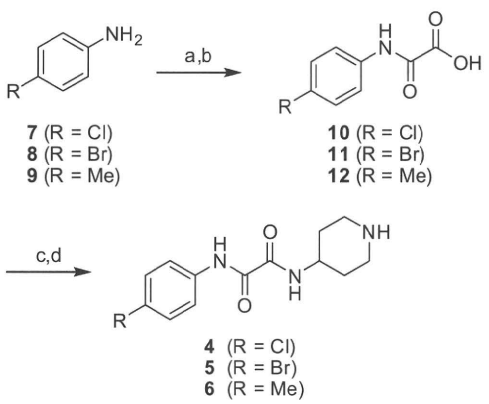

Scheme 1. Synthesis of compounds **4–6**. Reagents and conditions: (a) ethyl chloroglyoxylate, Et_3N, THF; (b) 1 M aq NaOH, THF, 67%–quant.; (c) 1-benzyl-4-aminopiperidine, EDC·HCl, HOBt·H_2O, Et_3N, THF; (d) (i) 1-chloroethyl chloroformate, CH_2Cl_2; (ii) MeOH, 8–47%.

Table 1
Effects of the methyl groups on anti-HIV activity and cytotoxicity of CD4 mimic analogs[a]

Compd	R	IC_{50} (μM) MNA (R5)	CC_{50} (μM)
1	Cl	12	110
2	Br	ND	93
3	Me	15	210
4	Cl	8	100
5	Br	6	50
6	Me	20	190

[a] All data with standard deviation are the mean values for at least three independent experiments (ND = not determined).

Compound **1** and the newly synthesized derivatives **4–6** were also evaluated for their effects on conformational changes of gp120 by a fluorescence activated cell sorting (FACS) analysis. The profile of binding of an anti-envelope CD4-induced monoclonal antibody (4C11) to the Env-expressing cell surface (an R5-HIV-1 strain, JR-FL, -infected PM1 cells) pretreated with the above derivatives was examined. Comparison of the binding of 4C11 to the cell surface was measured in terms of the mean fluorescence intensity (MFI), as shown in Figure 2. Pretreatment of the Env-expressing cell surface with compound **1** (MFI = 53.66) produced a significant increase in binding affinity for 4C11, consistent with that reported previously.[4e] This indicates that compound **1** enhances the binding affinity of gp120 with the 17b monoclonal antibody which recognizes CD4-induced epitopes on gp120. The Env-expressing cells without CD4 mimic-pretreatment failed to show significant binding affinity to 4C11. On the other hand, the profiles of the binding of 4C11 to the Env-expressing cell surface pretreated with compound **4** (Cl derivative) and **5** (Br derivative) (MFI = 49.88 and 52.34) were similar to that of compound **1**. Pretreatment of the cell surface with compound **6** (Me derivative) (MFI = 45.99) produced slightly lower enhancement but significant levels of binding affinity for 4C11, compared to that of compound **1** as pretreatments. These results suggested that the removal of the methyl groups on the piperidine moiety might not affect the CD4 mimicry effects on conformational changes of gp120 and it was conjectured that the phenyl ring of CD4 mimic might be a key moiety for the interaction with gp120 to induce the conformational changes of gp120. This is consistent with the results in the previous paper where it was reported that CD4 mimics having suitable substituent(s) on the phenyl ring cause a conformational change, resulting in external exposure of the co-receptor-binding site of gp120.[4e]

Based on these results, a series of N-alkylated and N-acylated piperidine derivatives **13–18** with no methyl groups were prepared. Several compounds with 6-membered rings were also prepared to determine whether or not the piperidine ring is mandatory. The synthesis of these derivatives is shown in Scheme 2. Since the *p*-Cl derivative **4** showed potent anti-HIV activity and relatively low cytotoxicity, compared to the *p*-Br derivative **5**, chlorine was selected as the substituent at the *p*-position of the phenyl ring. The N-methyl derivative **13** was synthesized by coupling of **10** with 4-amine-1-methylpiperidine. Alkylation of **4** with *tert*-butyl bromoacetate, followed by deprotection of *tert*-butyl ester provided compound **14**. The N-isopropyl derivative **15** was prepared by reductive amination of **4** with isopropyl aldehyde. The N-acyl derivatives **16–18** were prepared by simple acylation or condensation with the corresponding substrate. The synthesis of other derivatives **19–23** with different 6-membered rings is depicted in Scheme 3. The 6-membered ring derivatives with the exception of **21** were prepared by coupling of acid **10** with the corresponding amines. Compound **21** was prepared by reaction of **10** with thionyl chloride to give the corresponding acid chloride, which was subsequently coupled with 4-aminopyridine.

Compounds **1**, **3**, and **13–18** were evaluated for their CD4 mimicry effects on conformational changes of gp120 by the FACS anal-

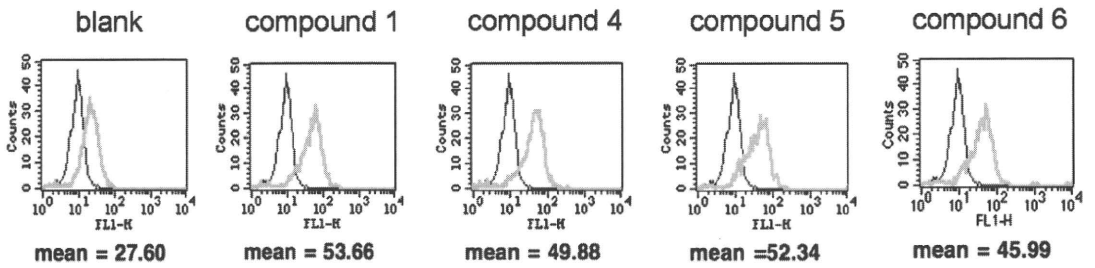

Figure 2. FACS analysis of compounds **1** and **4–6**. JR-FL (R5, Sub B) chronically infected PM1 cells were preincubated with 100 μM of a CD4 mimic for 15 min, and then incubated with an anti-HIV-1 mAb, 4C11, at 4 °C for 15 min. The cells were washed with PBS, and fluorescein isothiocyanate (FITC)-conjugated goat anti-human IgG antibody was used for antibody-staining. Flow cytometry data for the binding of 4C11 (green lines) to the Env-expressing cell surface in the presence of a CD4 mimic are shown among gated PM1 cells along with a control antibody (anti-human CD19:black lines). Data are representative of the results from a minimum of two independent experiments. The number at the bottom of each graph shows the mean fluorescence intensity (MFI) of the antibody 4C11.

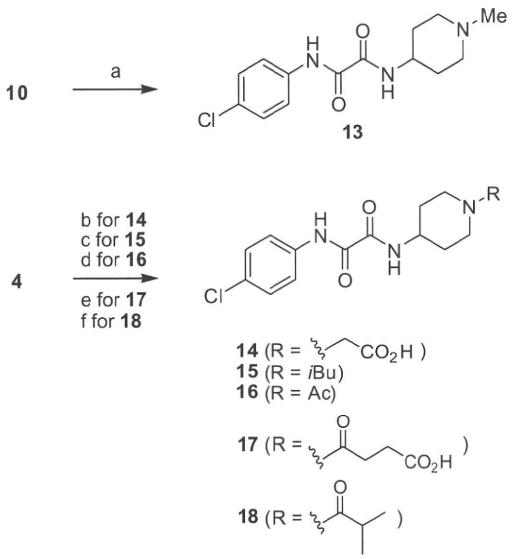

Scheme 2. Synthesis of N-alkylated and N-acylated piperidine derivatives **13–18**. Reagents and conditions: (a) 4-amine-1-methylpiperidine, EDC·HCl, HOBt·H_2O, Et_3N, THF, 16%; (b) (i) *tert*-butyl bromoacetate, NaH, DMF; (ii) TFA, 6%; (c) isobutylaldehyde, $NaBH(OAc)_3$, AcOH, DCE, quant.; (d) acetyl chloride, Et_3N, DMF, quant.; (e) succinic anhydride, Et_3N, THF, 37%; (f) isobutyric acid, EDC·HCl, HOBt·H_2O, Et_3N, THF, 95%.

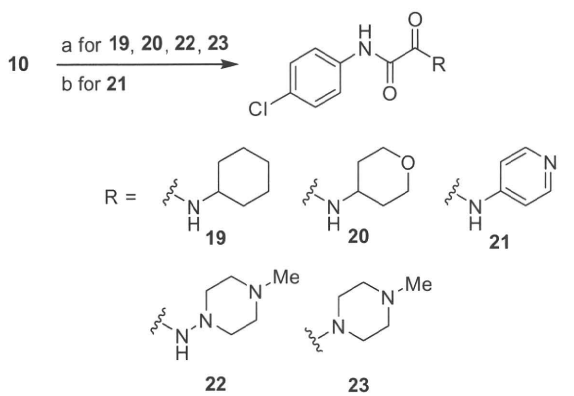

Scheme 3. Synthesis of 6-membered ring derivatives **19–23**. Reagents and conditions: (a) the corresponding amine, EDC·HCl, HOBt·H_2O, Et_3N, THF, 22%–quant.; (b) 4-aminopyridine, $SOCl_2$, MeOH, 38%.

ysis, and the results are shown in Figure 3. Pretreatment of the Env-expressing cells with the N-substituted compounds **13**, **15**, **16**, and **18** produced a notable increase in binding affinity to 4C11, similar to that observed in the pretreatment with compound **1**. The profile of the binding of 4C11 to the cell surface pretreated with compounds **14** and **17** was similar to that of controls, suggesting that these derivatives offer no significant enhancement of binding affinity for 4C11 and that the carboxylic moiety in the terminal of piperidine ring is not suited to CD4 mimicry. It is hypothesized that the carboxylic moieties of compounds **14** and **17** might prevent the interaction of CD4 mimic with gp120 by their multiple contacts with side chain(s) of amino acid(s) around the Phe43 cavity, such as Asp^{368} and Glu^{370}. Replacement of the piperidine moiety with the different 6-membered rings resulted in a significant loss of binding affinity for 4C11 in the FACS analysis of compound **19–23** (MFI(**19**) = 11.44, MFI(**20**) = 12.84, MFI(**21**) = 12.47, in MFI (blank) = 11.34; MFI(**22**) = 26.67, MFI(**23**) = 20.21, in MFI(blank) = 26.79, data not shown), indicating a significant contribution from the piperidine ring which interacts with gp120 inducing conformational changes.

In view of their ability to induce conformational changes of gp120, the anti-HIV activity and cytotoxicity of the piperidine derivatives **13–18** were further evaluated, with the results shown in Table 2. The anti-HIV activity of the synthetic compounds was evaluated against various viral strains including both laboratory and primary isolates and IC_{50} and CC_{50} values were determined as those of compounds **4–6**. The *N*-methylpiperidine compound **13**, was not found to possess significant anti-HIV activity against a primary isolate, but was found to possess moderate anti-HIV activity against a laboratory isolate, a IIIB strain (IC_{50} = 67 μM). Anti-HIV activity was not observed however, even at concentrations of 100 μM of **13** against an 89.6 strain. The potency was approximately eight-fold lower than that of the parent compound **1** (IC_{50} = 8 μM), indicating a partial contribution of the hydrogen atom of the amino group of the piperidine ring to the bioactivity of CD4 mimic. Although compound **15**, with an *N*-isobutylpiperidine moiety, failed to show significant anti-HIV activity against laboratory isolates, relativity potent activity was observed against a primary isolate, an MTA strain (IC_{50} = 28 μM). Compounds **16** and **18**, which are *N*-acylpiperidines, were tested against laboratory isolates and significant anti-HIV activity was not observed even at 100 μM. Compounds **14** and **17**, with the carboxylic moieties, failed to show significant anti-HIV activity against laboratory isolates even at 100 μM, which are compatible with the FACS analysis. These results suggest that the N-substituent on the piperidine ring of CD4 mimic analogs may contribute to a critical interaction required for binding to gp120. Compounds **19–23** showed no significant anti-HIV activity against a IIIB strain even at 100 μM, which are compatible with the FACS analysis (data not shown).

All but one of the compounds **13–18** have no significant cytotoxicity to PM1/CCR5 cells ($CC_{50} \geqslant 260$ μM); the exception is compound **18** (CC_{50} = 45 μM). Compounds **13** and **15** show relatively potent anti-HIV activity without significant cytotoxicity.

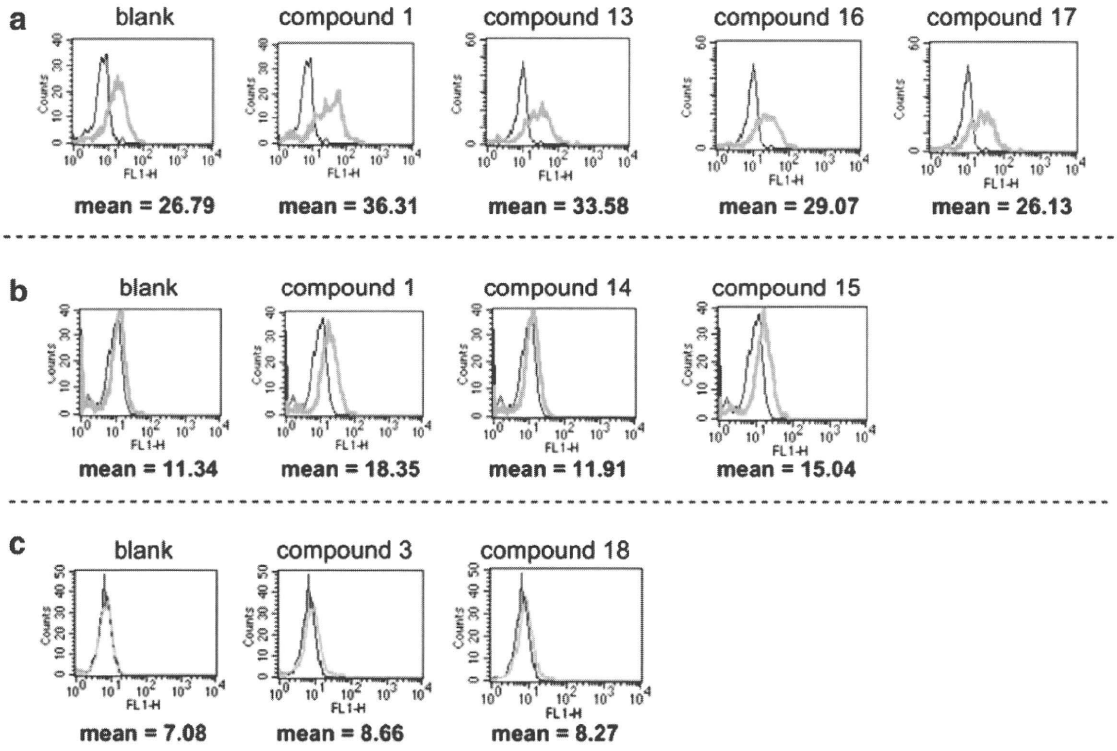

Figure 3. FACS analysis of compounds **1**, **3**, and **13–18**. The experimental procedures are described in Figure 2. The lanes of (a), (b) and (c) show independent experiments.

Table 2
Anti-HIV activity and cytotoxicity of compounds **13–18**[a]

Compd	R	IC_{50} (μM)			CC_{50} (μM)
		Laboratory isolates		Primary isolates	
		IIIB (X4)	89.6 (dual)	MTA (R5)	
1		8	10	ND	150
4	H	ND	ND	ND	100
13	Me	67	>100	ND	>300
14	CH_2CO_2H	>100	ND	ND	260
15	*i*Bu	>100	ND	28	>300
16	Ac	>100	>100	ND	>300
17	$C(O)CH_2CH_2CO_2H$	>100	>100	ND	>300
18	C(O)*i*Pr	>100	ND	ND	45

[a] All data with standard deviation are the mean values for at least three independent experiments.

The results for **15** showed it to have 3–6 times less cytotoxicity than **4** and **18**. This observation indicates that the alkylation of the piperidine nitrogen may be favorable because it lowers the cytotoxicity of CD4 mimic analogs.

In the course of the SAR studies on CD4 mimic analogs, we have already found that a CD4 mimic or sCD4 exhibited a remarkable synergistic effect[4e] with a 14-mer peptide CXCR4 antagonist T140.[9] This result indicates that the interaction of CD4 mimic with gp120 could facilitate the approach of CXCR4 to gp120 by exposing the co-receptor binding site of gp120. It was thought that the CD4 mimic analogs conjugated with a selective CXCR4 antagonist might as a consequence show a higher synergistic effect for the improvement of anti-HIV activity. In this context, efforts were made to synthesize and bioevaluate hybrid molecules that combined a CD4 mimic analog with 4F-benzoyl-TZ14011, which is a derivative of T140 optimized for CXCR4 binding and stability in vivo.[10]

The synthesis of hybrid molecules **27–29** is outlined in Scheme 4. To examine the influence of the linker length on anti-HIV activity and cytotoxicity, three hybrid molecules with linkers of different lengths were designed. Based on the fact that alkylation of the piperidine nitrogen, having no deleterious effects on bioactivity, is an acceptable modification of CD4 mimic analogs, the alkylamine moiety was incorporated into the nitrogen atom of the piperidine moiety to conjugate CD4 mimic analogs with 4F-benzoyl-TZ14011. Reductive alkylation of **4** with N^{α}-Boc-pyrrolidin-2-ol **24**, which exists in equilibrium with the corresponding aldehyde, and successive treatment with TFA and HCl/dioxane provided the amine hydrochloride **25**. Treatment of **25** with succinic anhydride under basic condition gave the corresponding acid **26**, which was subjected to condensation with the side chain of D-Lys[8] of 4F-benzoyl-TZ14011 in an EDC–HOBt system to give the desired hybrid molecule **27** with a tetramethylene linker.[11] Other hybrid molecules **28** and **29** bearing hexa- and octamethylene linkers, respectively, were prepared using the corresponding aldehydes **30** and **31**.

The assay results for these hybrid molecules **27–29** are shown in Table 3. To investigate the effect of conjugation of two molecules on binding activity against CXCR4, the inhibitory potency against

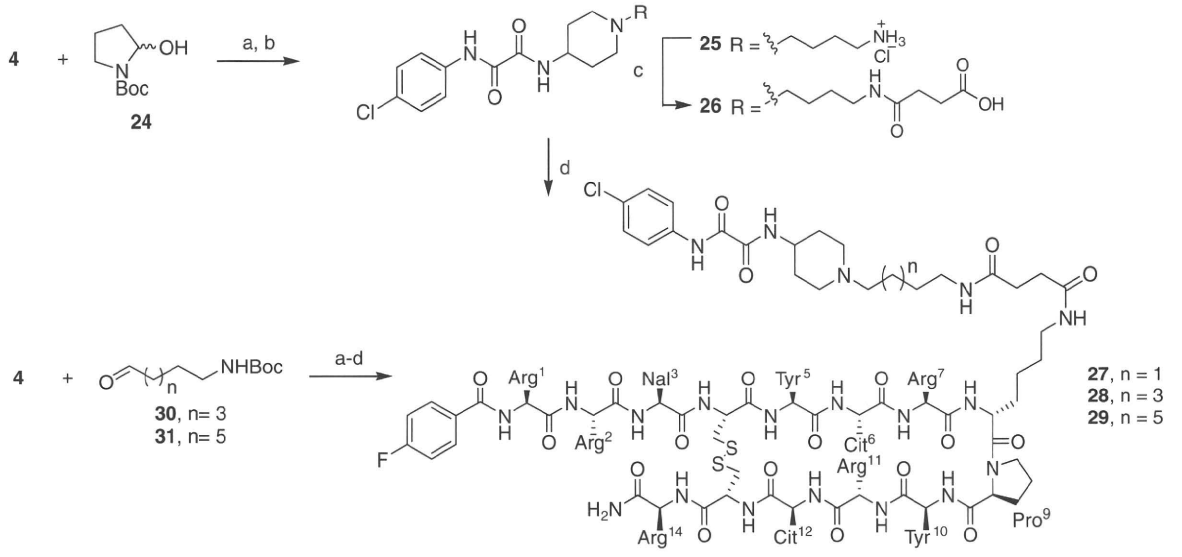

Scheme 4. Synthesis of hybrid molecules **27–29**. Reagents and conditions: (a) $NaBH(OAc)_3$, AcOH, DCE; (b) TFA, then 4 M HCl/1,4-dioxane; (c) succinic anhydride, pyridine, DMF, then 4 M HCl/1,4-dioxane; (d) 4F-benzoyl-TZ14011, EDC·HCl, HOBt·H_2O, Et_3N, DMF. Nal = L-3-(2-naphthyl)alanine, Cit = L-citrulline.

Table 3
CXCR4-binding activity, anti-HIV activity and cytotoxicity of hybrid molecules **27–29**[a]

Compd	EC_{50}[b] (μM)	IC_{50}[c] (μM)	CC_{50}[d] (μM)	SI (CC_{50}/IC_{50})
4F-benzoyl-TZ14011	0.0059	0.0131	ND	ND
1 (NBD-556)	ND	0 2.10	ND	19.2[e]
27 (C4)	0.0044	0.0509	8.60	169
28 (C6)	0.0187	0.0365	8.00	219
29 (C8)	0.0071	0.0353	8.60	244
AZT	ND	0.0493	ND	ND

[a] All data with standard deviation are the mean values for at least three independent experiments.

[b] EC_{50} values are based on the inhibition of [^{125}I]-SDF-1α binding to CXCR4 transfectants of CHO cells.

[c] IC_{50} values are based on the inhibition of HIV-1-induced cytopathogenicity in MT-2 cells.

[d] CC_{50} values are based on the reduction of the viability of mock-infected MT-2 cells.

[e] This value is based on the CC_{50} and IC_{50} values from Table 1.

binding of [^{125}I]-SDF-1α to CXCR4 was measured. All the hybrid molecules **27–29** significantly inhibited the SDF-1α binding to CXCR4. The corresponding EC_{50} values are: EC_{50}(**27**) = 0.0044 μM; EC_{50}(**28**) = 0.0187 μM; EC_{50}(**29**) = 0.0071 μM. These potencies are comparable to that of 4F-benzoyl-TZ14011 (EC_{50} = 0.0059 μM), indicating that introduction of the CD4 mimic analog into the D-Lys[8] residue of 4F-benzoyl-TZ14011 does not affect binding activity against CXCR4. Comparison of the binding activities of **27–29** showed that all hybrid molecules were essentially equipotent in inhibition of the binding of SDF-1α to CXCR4. This observation indicates that the linker length between two molecules has no effect on the binding inhibition.

Anti-HIV activity based on the inhibition of HIV-1 entry into the target cells was examined by the MTT assay using a IIIB(X4) strain. In this assay, the IC_{50} value of 4F-benzoyl-TZ14011 was 0.0131 μM. All hybrid molecules **27–29** showed significant anti-HIV activity [IC_{50}(**27**) = 0.0509 μM; IC_{50}(**28**) = 0.0365 μM; IC_{50}(**29**) = 0.0353 μM]; however, the potency was 2- to 4-fold lower than that of the parent compound 4F-benzoyl-TZ14011, indicating that the conjugation of CD4 mimic with a CXCR4 antagonist did not provide a significant synergistic effect. In view of the fact that the combinational uses of CD4 mimic with T140 produced a highly remarkable synergistic effect, the lower potency of hybrid molecules may be attributed to the inadequacy in the structure and/or the characters of the linkers. All the hybrid molecules **27–29** have relatively strong cytotoxicity [CC_{50}(**27**) = 8.6 μM; CC_{50}(**28**) = 8.0 μM; CC_{50}(**29**) = 8.6 μM]. However, selectivity indexes (SI = CC_{50}/IC_{50}) were 169 for **27**, 219 for **28**, and 244 for **29**, all 9–13 times higher than that of **1** (SI = 9.2). This result indicates that conjugation of a CD4 mimic analog with a selective CXCR4 antagonist can improve the SI of CD4 mimic.

The SAR study of a series of CD4 mimic analogs was conducted to investigate the contribution of the piperidine moiety of **1** to anti-HIV activity, cytotoxicity, and CD4 mimicry on conformational changes of gp120. The results indicate that (i) the methyl groups on the piperidine ring of **1** have no great influence on the activities of CD4 mimic; (ii) the presence of piperidine moiety is important for the CD4 mimicry; and (iii) N-substituents of the piperidine moiety contribute significantly to anti-HIV activity and cytotoxicity, as observed with N-alkyl groups such as methyl and isobutyl groups which show moderate anti-HIV activity and lower cytotoxicity.

Several hybrid molecules based on conjugation of a CD4 mimic with a selective CXCR4 antagonist were also synthesized and bioevaluated. All the hybrid molecules showed significant binding activity against CXCR4 comparable to the parent antagonist and exhibited potent anti-HIV activity. Although no significant synergistic effect was observed, conjugation of a CD4 mimic with a selective CXCR4 antagonist might lead to the development of novel type of CD4 mimic-based HIV-1 entry inhibitors, which possess higher selective indexes than a simple CD4 mimic. These results will be useful for the rational design and synthesis of a new type of HIV-1 entry inhibitors. Further structural modification studies of CD4 mimic are the subject of an ongoing project.

Acknowledgements

This work was supported by Grant-in-Aid for Scientific Research from the Ministry of Education, Culture, Sports, Science, and Technology of Japan, Japan Human Science Foundation, and Health and Labour Sciences Research Grants from Japanese Ministry of Health, Labor, and Welfare. T.T. and N.O. are grateful for the JSPS Reseach Fellowships for Young Scientist.

References and notes

1. Chan, D. C.; Kim, P. S. *Cell* **1998**, *93*, 681.
2. (a) Alkhatib, G.; Combadiere, C.; Broder, C. C.; Feng, Y.; Kennedy, P. E.; Murphy, P. M.; Berger, E. A. *Science* **1996**, *272*, 1955; (b) Choe, H.; Farzan, M.; Sun, Y.; Sullivan, N.; Rollins, B.; Ponath, P. D.; Wu, L.; Mackay, C. R.; LaRosa, G.; Newman, W.; Gerard, N.; Gerard, C.; Sodroski, J. *Cell* **1996**, *85*, 1135; (c) Deng, H. K.; Liu, R.; Ellmeier, W.; Choe, S.; Unutmaz, D.; Burkhart, M.; Marzio, P. D.; Marmon, S.; Sutton, R. E.; Hill, C. M.; Davis, C. B.; Peiper, S. C.; Schall, T. J.; Littman, D. R.; Landau, N. R. *Nature* **1996**, *381*, 661; (d) Doranz, B. J.; Rucker, J.; Yi, Y. J.; Smyth, R. J.; Samson, M.; Peiper, S. C.; Parmentier, M.; Collman, R. G.; Doms, R. W. *Cell* **1996**, *85*, 1149; (e) Dragic, T.; Litwin, V.; Allaway, G. P.; Martin, S. R.; Huang, Y.; Nagashima, K. A.; Cayanan, C.; Maddon, P. J.; Koup, R. A.; Moore, J. P.; Paxton, W. A. *Nature* **1996**, *381*, 667.
3. Feng, Y.; Broder, C. C.; Kennedy, P. E.; Berger, E. A. *Science* **1996**, *272*, 872.
4. (a) Zhao, Q.; Ma, L.; Jiang, S.; Lu, H.; Liu, S.; He, Y.; Strick, N.; Neamati, N.; Debnath, A. K. *Virology* **2005**, *339*, 213; (b) Schön, A.; Madani, N.; Klein, J. C.; Hubicki, A.; Ng, D.; Yang, X.; Smith, A. B., III; Sodroski, J.; Freire, E. *Biochemistry* **2006**, *45*, 10973; (c) Madani, N.; Schön, A.; Princiotto, A. M.; LaLonde, J. M.; Courter, J. R.; Soeta, T.; Ng, D.; Wang, L.; Brower, E. T.; Xiang, S.-H.; Do Kwon, Y.; Huang, C.-C.; Wyatt, R.; Kwong, P. D.; Freire, E.; Smith, A. B., III; Sodroski, J. *Structure* **2008**, *16*, 1689; (d) Haim, H.; Si, Z.; Madani, N.; Wang, L.; Courter, J. R.; Princiotto, A.; Kassa, A.; DeGrace, M.; McGee-Estrada, K.; Mefford, M.; Gabuzda, D., ; Smith, A. B., III; Sodroski, J. *ProS Pathogens* **2009**, *5*, 1; (e) Yamada, Y.; Ochiai, C.; Yoshimura, K.; Tanaka, T.; Ohashi, N.; Narumi, T.; Nomura, W.; Harada, S.; Matsushita, S.; Tamamura, H. *Bioorg. Med. Chem. Lett.* **2010**, *20*, 354; (f) Yoshimura, K.; Harada, S.; Shibata, J.; Hatada, M.; Yamada, Y.; Ochiai, C.; Tamamura, H.; Matsushita, S. *J. Virol.* **2010**, *84*, 7558.
5. Protein Data Bank (PDB) (entry 1RZJ).
6. Olofson, R. A.; Abbott, D. E. *J. Org. Chem.* **1984**, *49*, 2795.
7. The synthesis of compound **4**: To the solution of compound **10** (104 mg, 0.52 mmol) in dry THF (4.0 mL), Et_3N (159 μL, 1.15 mmol), HOBt·H_2O (87 mg, 0.57 mmol), EDCI·HCl (109 mg, 0.57 mmol) and 4-amino-1-benzylpiperidine (109 μL, 0.57 mmol) were added with stirring at 0 °C, and continuously stirred for 6 h with warming to room temperature under N_2 atmosphere. After concentration under reduced pressure, the residue was extracted with EtOAc. The extract was washed with aq saturated $NaHCO_3$ and brine, and dried over $MgSO_4$. Concentration under reduced pressure followed by flash chromatography over silica gel with $CHCl_3$–MeOH (20:1) including 1% Et_3N gave the crude benzyl amine as a white powder. To the solution of the above crude benzyl amine (95 mg, 0.26 mmol) in dry CH_2Cl_2 (10 mL), 1-chloroethyl chloroformate (110 μL, 0.68 mmol) was added dropwise with stirring at 0 °C. The mixture was then refluxed for 3 h under N_2 atmosphere. After concentration under reduced pressure, the residue was resolved in MeOH (10 mL) and then refluxed for 1 h. Concentration under reduced pressure gave a crude product. Reprecipitation with MeOH–Et_2O afforded a white powder of the title compound **4** (33 mg, 46% yield). δ_H(400 MHz; CD_3OD) 1.83–1.92 (2H, m, CH_2), 2.10–2.17 (2H, m, CH_2), 3.13 (2H, t, *J* 12.5, CH_2), 3.34 (1H, m, NH), 3.42–3.49 (1H, m, CH_2), 4.04 (1H, m, CH), 7.34 (2H, m, ArH), 7.51 (1H, m, NH), 7.73 (2H, m, ArH), 8.84 (1H, m, NH); LRMS (ESI), *m/z* calcd for $C_{13}H_{17}ClN_3O_2$ $(MH)^+$ 282.10, found 282.14.
8. Yoshimura, K.; Shibata, J.; Kimura, T.; Honda, A.; Maeda, Y.; Koito, A.; Murakami, T.; Mitsuya, H.; Matsushita, S. *AIDS* **2006**, *20*, 2065.
9. (a) Tamamura, H.; Xu, Y.; Hattori, T.; Zhang, X.; Arakaki, R.; Kanbara, K.; Omagari, A.; Otaka, A.; Ibuka, T.; Yamamoto, N.; Nakashima, H.; Fujii, N. *Biochem. Biophys. Res. Commun.* **1998**, *253*, 877; (b) Tamamura, H.; Hiramatsu, K.; Mizumoto, M.; Ueda, S.; Kusano, S.; Terakubo, S.; Akamatsu, M.; Yamamoto, N.; Trent, J. O.; Wang, Z.; Peiper, S. C.; Nakashima, H.; Otaka, A.; Fujii, N. *Org. Biomol. Chem.* **2003**, *1*, 3663.
10. Hanaoka, H.; Mukai, T.; Tamamura, H.; Mori, T.; Ishino, S.; Ogawa, K.; Iida, Y.; Doi, R.; Fujii, N.; Saji, H. *Nucl. Med. Biol.* **2006**, *33*, 489.
11. The synthesis of a hybrid molecule **27**: To the solution of compound **26** (2.6 mg, 4.6 μmol) in DMF (1.0 mL), Et_3N (26 μL, 92 μmol), HOBt·H_2O (3.5 mg, 23 μmol) and EDCI·HCl (4.5 mg, 23 μmol) were added with stirring at 0 °C, and stirred for 1 h at room temperature. To the mixture 4F-benzoyl-TZ14011 (15 mg, 4.1 μmol) was then added and the mixture was stirred for 24 h at room temperature under N_2 atmosphere. After concentration under reduced pressure, the residue was purified by reversed phase HPLC (t_R = 23 min, elution: a linear gradient of 27–31% acetonitrile containing 0.1% TFA over 30 min) to afford a fluffy white powder of the desired compound **27** (1.3 mg, 9.8%). LRMS (ESI), *m/z* 2621.20 $[M+H]^+$, calcd 2620.25.

JOURNAL OF VIROLOGY, Aug. 2010, p. 7558–7568 Vol. 84, No. 15
0022-538X/10/$12.00 doi:10.1128/JVI.00227-10

Enhanced Exposure of Human Immunodeficiency Virus Type 1 Primary Isolate Neutralization Epitopes through Binding of CD4 Mimetic Compounds[▽]

Kazuhisa Yoshimura,[1] Shigeyoshi Harada,[1] Junji Shibata,[1] Makiko Hatada,[1] Yuko Yamada,[2] Chihiro Ochiai,[2] Hirokazu Tamamura,[2] and Shuzo Matsushita[1]*

Division of Clinical Retrovirology and Infectious Diseases, Center for AIDS Research, Kumamoto University, Kumamoto, Japan,[1] and Institute of Biomaterials and Bioengineering, Tokyo Medical and Dental University, Chiyoda-ku, Tokyo, Japan[2]

Received 17 March 2010/Accepted 13 May 2010

***N*-(4-Chlorophenyl)-*N'*-(2,2,6,6-tetramethyl-piperidin-4-yl)-oxalamide (NBD-556) is a low-molecular-weight compound that reportedly blocks the interaction between human immunodeficiency virus type 1 (HIV-1) gp120 and its receptor CD4. We investigated whether the enhancement of binding of anti-gp120 monoclonal antibodies (MAbs) toward envelope (Env) protein with NBD-556 are similar to those of soluble CD4 (sCD4) by comparing the binding profiles of the individual MAbs to Env-expressing cell surfaces. In flow cytometric analyses, the binding profiles of anti-CD4-induced epitope (CD4i) MAbs toward NBD-556-pretreated Env-expressing cell surfaces were similar to the binding profiles toward sCD4-pretreated cell surfaces. To investigate the binding position of NBD-556 on gp120, we induced HIV-1 variants that were resistant to NBD-556 and sCD4 *in vitro*. At passage 21 in the presence of 50 μM NBD-556, two amino acid substitutions (S375N in C3 and A433T in C4) were identified. On the other hand, in the selection with sCD4, seven mutations (E211G, P212L, V255E, N280K, S375N, G380R, and G431E) appeared during the passages. The profiles of the mutations after the selections with NBD-556 and sCD4 were very similar in their three-dimensional positions. Moreover, combinations of NBD-556 with anti-gp120 MAbs showed highly synergistic interactions against HIV-1. We further found that after enhancing the neutralizing activity by adding NBD-556, the contemporaneous virus became highly sensitive to antibodies in the patient's plasma. These findings suggest that small compounds such as NBDs may enhance the neutralizing activities of CD4i and anti-V3 antibodies *in vivo*.**

Human immunodeficiency virus type 1 (HIV-1) replicates continuously in the face of a strong antibody (Ab) response, although Abs effectively control many viral infections (3). Neutralizing Abs (NAbs) are directed against the HIV-1 envelope (Env) protein, which is a heterodimer comprising an extensively glycosylated CD4-binding subunit (gp120) and an associated transmembrane protein (gp41). Env proteins are present on the virion surface as "spikes" composed of trimers of three gp120-gp41 complexes (20, 21, 29). These spikes resist neutralization through epitope occlusion within the oligomer, extensive glycosylation, extension of variable loops from the surface of the complex, and steric and conformational blocking of receptor binding sites (16, 18, 20).

Ab access to conserved regions is further limited because viral entry is a stepwise process involving conformational changes that lead to only transient exposure of conserved domains such as the coreceptor binding site (4, 5). However, some early strains of HIV-1 appear to be highly susceptible to neutralization by Abs (1, 10). For instance, subtype A HIV-1 envelopes from the early stage of infection exhibit a broad range of neutralization sensitivities to both autologous and heterologous plasma (1), suggesting that at least a subset of the envelopes have some preserved and/or exposed neutralization epitopes. It is well known that the potential for neutralizing properties of particular Abs is enhanced after binding of soluble CD4 (sCD4), especially NAbs against CD4-induced epitopes (CD4i Abs) (27) and some anti-V3 Abs (22). CD4i Abs are detected in plasma samples from many patients at an early stage of HIV-1 infection (9). Consequently, we hypothesize that small compounds such as sCD4 can enhance the neutralizing activities of CD4i Abs and some anti-V3 Abs not only *in vitro* but also *in vivo*.

In a previous report, two low-molecular-weight compounds that presumably interfere with viral entry of HIV-1 into cells were described (35). These two *N*-phenyl-*N'*-(2,2,6,6-tetramethyl-piperidin-4-yl)-oxalamide analogs, NBD-556 and NBD-557, comprise a novel class of HIV-1 entry inhibitors that block the interaction between gp120 and CD4. These compounds were found to be equally potent inhibitors of both X4 and R5 viruses in CXCR4- and CCR5-expressing cell lines, respectively (35). Schön et al. (25) also reported that NBD-556 binds to gp120 in a process characterized by a large favorable change in enthalpy that is partially compensated for by a large unfavorable entropy change, representing a thermodynamic signature similar to that observed for binding of sCD4 to gp120. In a recent study, Madani et al. (23) reported the following findings: (i) NBD-556 binds within the Phe43 cavity, a highly conserved and functionally important pocket formed as gp120 assumes the CD4-bound conformation; (ii) the NBD-556 phenyl ring projects into the Phe43 cavity; (iii) the enhancement of CD4-independent infection by NBD-556 requires the induction of conformational changes in gp120; and (iv) increased

* Corresponding author. Mailing address: Division of Clinical Retrovirology and Infectious Diseases, Center for AIDS Research, Kumamoto University, Kumamoto 860-0811, Japan. Phone: 81-96-373-6536. Fax: 81-96-373-6537. E-mail: shuzo@kumamoto-u.ac.jp.

▽ Published ahead of print on 26 May 2010.

affinities of NBD-556 analogs toward gp120 improve the antiviral potency during infection of CD4-expressing cells. The latter two studies demonstrated that low-molecular-weight compounds such as NBDs can induce conformational changes in the HIV-1 gp120 glycoprotein similar to those observed upon sCD4 binding (23, 25). The authors of these studies concluded that their data supported the importance of gp120 residues near the Phe43 cavity in binding to NBD-556 and lent credence to the docked binding mode.

In the present study, we investigated the binding position of NBD-556 on gp120 by inducing HIV-1 variants that were resistant to NBD-556 by exposing HIV-1_{IIIB} to increasing concentrations of the compound *in vitro*. We also induced sCD4-resistant HIV-1_{IIIB} variants and compared the profile of the sCD4-resistant mutations to that of the NBD-556-resistant mutations. We subsequently examined the virological properties of pseudotyped HIV-1 clones carrying the NBD-556 and sCD4 resistance-associated *env* gene mutations. Our findings provide a foundation for understanding the interaction of NBD-556 with the CD4-binding site of HIV-1 gp120. We also evaluated the anti-HIV-1 interactions between plasma NAbs and NBD-556 *in vitro* and considered the possibility of using the data as a key to opening the shield covering the conserved epitopes targeted by NAbs.

(This study was presented in part at the 15th Conference on Retroviruses and Opportunistic Infection, Boston, MA, 3 to 6 February 2008 [Abstract 736].)

MATERIALS AND METHODS

Cells, culture conditions, and reagents. The CD4-positive T-cell line PM1 was maintained in RPMI 1640 (Sigma, St. Louis, MO) supplemented with 10% heat-inactivated fetal calf serum (FCS; HyClone Laboratories, Logan, UT), 50 U of penicillin/ml, and 50 μg of streptomycin/ml. PM1/CCR5 cells were generated by standard retrovirus-mediated transduction of PM1 cells with pBABE-CCR5 provided by the National Institutes of Health AIDS Research and Preference Reagent Program (NIH ARRRP) (24, 34). PM1/CCR5 cells were maintained in RPMI 1640 supplemented with 10% heat-inactivated FCS, 50 U of penicillin/ml, 50 μg of streptomycin/ml, and 0.1 mg of G418 (Invitrogen, Carlsbad, CA)/ml. The TZM-bl cell line was obtained from the NIH ARRRP and maintained in Dulbecco modified Eagle medium (Sigma) supplemented with 10% FCS.

NBD-556 (molecular weight, 337.84) and YYA-004 (molecular weight, 303.4), which has the same structure as JRC-I-300 (23), were synthesized as previously described (23, 25, 30). KD-247 (12), 3E4, and 0.5γ (unpublished) are anti-gp120-V3 monoclonal Abs (MAbs). 17b (27), 4C11, and 4E9C (unpublished) are MAbs against CD4-induced epitopes (CD4i Abs). 17b, 2G12 (a MAb against the gp120 glycan), and b12 (a MAb against the CD4-binding site [CD4bs] epitope) were provided by the NIH ARRRP. The 0.5δ antibody established in our laboratory is an anti-CD4bs MAb (unpublished results). RPA-T4 (an anti-CD4 MAb) was purchased from BD Biosciences Pharmingen (San Jose, CA). Recombinant human sCD4 was purchased from R&D Systems, Inc. (Minneapolis, MN).

MAbs 3E4, 0.5γ, 0.5δ, 4C11, and 4E9C were human MAbs established from a patient with long-term nonprogressive illness. B cells from the patient's peripheral blood mononuclear cells (PBMC) were transformed by Epstein-Barr virus, followed by cloning. Culture supernatant from an individual clone was screened for reactivity to $gp120_{SF2}$ by enzyme-linked immunosorbent assay (ELISA). The specificity of the antibodies was determined by gp120 capture ELISA and fluorescence-activated cell sorting analysis of HIV-1_{JR-FL}-infected PM1 cells in the presence or absence of sCD4. The binding specificity was further assessed by an ELISA using peptides corresponding to the V3 sequence of various isolates. Based on these binding data, we classified them as follows: V3 MAbs, 3E4 and 0.5γ; CD4bs MAb, 0.5δ; and CD4i MAbs, 4C11 and 4E9C.

The laboratory-adapted HIV-1 strains HIV-$1_{89.6}$, HIV-1_{BaL}, HIV-1_{SF162}, HIV-1_{JR-FL}, and HIV-1_{YU2} were propagated in phytohemagglutinin-activated PBMC. These viruses were then passaged in PM1/CCR5 cells, and the culture supernatants were stored at −150°C prior to use. R5 primary HIV-1 isolates (HIV-$1_{Pt.1}$, HIV-$1_{Pt.2}$, HIV-$1_{Pt.3}$, and HIV-$1_{Pt.4}$) were isolated from four Japanese patients in our laboratory. All patients were at a stage of chronic infection. HIV-$1_{Pt.1}$, HIV-$1_{Pt.3}$, and HIV-$1_{Pt.4}$ were isolated from drug-naive patients, and HIV-$1_{Pt.2}$ was isolated from a drug-experienced patient and passaged in phytohemagglutinin-activated PBMC. Infected PBMC were cocultured with PM1/CCR5 cells for 4 to 5 days, and the culture supernatants were stored at −150°C until used. Nucleotide sequences of the gp120 from the four primary isolates were deposited in the DNA Data Bank of Japan under accession numbers AB553911 to AB553914.

Susceptibility assay. The sensitivities of six laboratory-adapted viruses, four primary isolates, and HIV-1_{IIIB} viruses passaged in the presence of sCD4 or NBD-556 were determined by the MTT [3-(4,5-dimethylthiazol-2-yl)-2,5-diphenyltetrazolium bromide] assay as previously described with minor modifications (31). Briefly, PM1/CCR5 cells (2×10^3 cells/well) were exposed to 100 times the 50% tissue culture infective dose ($TCID_{50}$) of the viruses in the presence of various concentrations of sCD4 or NBD-556 in 96-well round-bottom microculture plates, followed by incubation at 37°C for 7 days. After removal of 100 μl of the medium, 10 μl of MTT solution (7.5 mg/ml) in phosphate-buffered saline (PBS) was added to each well. The plate was then incubated at 37°C for 3 h. Subsequently, the produced formazan crystals were dissolved by adding 100 μl of acidified isopropanol containing 4% (vol/vol) Triton X-100 to each well. The optical densities at a wavelength of 570 nm were measured in a microplate reader. All assays were performed in duplicate or triplicate. We also determined the concentration for 50% cytotoxicity (CC_{50}) by using the MTT assay.

The sensitivities of the HIV-$1_{Pt.3}$ primary isolate to KD-247 (anti-V3 MAb), 4E9C (CD4i MAb), and autologous plasma IgG in the presence or absence of NBD-556 were also determined by using the MTT assay. To exclude any influence of plasma factors, such as antiviral drugs, cytokines, and chemokines, on the neutralization activities, we used IgG from the patient's plasma, which was purified using protein A-Sepharose (Affi-gel Protein A; Bio-Rad, Hercules, CA) (19).

Flow cytometric analysis. HIV-1_{JR-FL} chronically infected PM1 cells were preincubated with or without sCD4 (0.5 μg/ml) and NBD-556 (1, 3, 10, 30, 90, and 100 μM) for 15 min and then incubated with various anti-HIV-1 MAbs (17b, 4C11, KD-247, 3E4, and 0.5γ) at 4°C for 30 min. The cells were washed with PBS, and a fluorescein isothiocyanate-conjugated goat anti-human IgG Ab was used for Ab detection. Flow cytometry was performed with a FACSCalibur flow cytometer (BD Biosciences), and the data were analyzed by using the BD CellQuest version 3.1 software (BD Biosciences).

Data analysis and evaluation of synergy. Analyses of the synergistic, additive, and antagonistic effects of the antiviral agents were initially performed according to the median effect principle using the CalcuSyn version 2 computer program (6) to provide estimates of the 50% inhibitory concentration (IC_{50}) values of the antiviral agents in combination. Combination indices (CIs) were estimated from the data and reflected the nature of the interactions between KD-247 and sCD4 or NBD-556 and between NBD-556 and CD4i MAb 4C11 or anti-CD4bs MAb 0.5δ against HIV-1_{JR-FL} or HIV-1_{IIIB} on PM1/CCR5 cells as determined by the MTT assay. A CI of <0.9 indicated synergy, a CI between 0.9 and 1.1 indicated additivity, and a CI of >1.1 indicated antagonism. The CI value was directly proportional to the amount of synergy for the combination regimen. For example, values of <0.5 represented a high degree of synergy, while values of >1.5 represented significant antagonism. This approach has been widely used in analyses of antiviral interactions and was chosen to allow comparability with published literature.

Docking simulation. The structure for NBD-556 was built in SYBYL 7.1 (Tripos, St. Louis, MO) and minimized with the MMFF94 force field and partial charges (15). Using FlexSIS through its SYBYL module, docking of NBD-556 was performed into the crystal structure of gp120 obtained from the Protein Data Bank (PDB; entry 1RZJ). The binding site was defined as residues Val255, Asp368, Glu370, Ser375, Ile424, Trp427, Val430, and Val475, including residues located within a radius of 4.4 Å. The structure of the ligand was treated flexibly, and all other options were set to their default values. Figures were generated using SwissPdb Viewer version 3.9 (SPdbViewer) (13) and ViewerLite version 5.0 (Accelrys, Inc., San Diego, CA). We also generated a simian immunodeficiency virus (SIV) gp120 figure (PDB entry 2BF1) to compare the sites of the mutations in HIV-1 gp120 using the same software programs.

Isolation of NBD-556- and sCD4-resistant mutants from HIV-1_{IIIB} *in vitro*. To select NBD-556 and sCD4 escape viruses, HIV-1_{IIIB} was treated with various concentrations of NBD-556 or sCD4 and then infected into PM1/CCR5 cells as previously described with minor modifications (32). Viral replication was monitored by observation of any cytopathic effects in PM1/CCR5 cells. The culture supernatants were harvested on day 7 and used to infect fresh PM1/

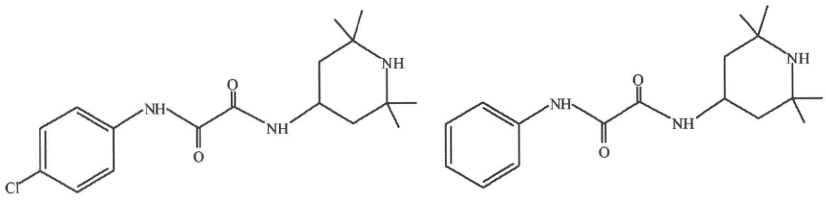

NBD-556 YYA-004

FIG. 1. Structures of NBD-556 and YYA-004.

CCR5 cells for the next round of culture in the presence of increasing concentrations of NBD-556 or sCD4. When the viruses began to propagate in the presence of NBD-556 or sCD4, the concentration was further increased. After the viruses were passaged using up to 50 μM NBD-556 or 20 μg of sCD4/ml in PM1/CCR5 cells, the resulting viruses, designated NBD-556(20)14p, NBD-556(50)17p, and sCD4(20)5p, were recovered from the passaged cell culture supernatants.

Proviral DNA extracts from cells cultured with several concentrations of NBD-556 and sCD4 were subjected to PCR amplification using *Taq* polymerase (Takara, Shiga, Japan). The amplified products were cloned into pCR2.1 (Invitrogen), and the *env* regions in both the passaged and selected viruses were sequenced by using an ABI Prism 3110 automated DNA sequencer (ABI, Foster City, CA).

Construction of mutant Env expression vectors. Proviral DNA was extracted from the passaged HIV-1_{IIIB}-infected PM1/CCR5 cells by using a QIAamp DNA blood minikit (Qiagen, Valencia, CA). For the construction of Env expression vectors, we used pCXN2, which contains a chicken actin promoter. Briefly, we amplified the passaged HIV-1_{IIIB} gp160 regions using LA *Taq* (Takara) with the primers ENVA (5′-GGCTTAGGCATCTCCTATGGCAGGAAGAA-3′) and ENVN (5′-CTGCCAATCAGGGAAGTAGCCTTGTGT-3′). The PCR products were inserted into pCR-XL-TOPO (Invitrogen). The EcoRI fragment of pCR-XL-IIIB containing the entire *env* region was ligated into pCXN2 to give pCXN-IIIBwt. pCXN-IIIB(S375N), pCXN-IIIB(V255E), and pCXN-IIIB(A433T) were generated by site-directed mutagenesis using a QuikChange site-directed mutagenesis kit (Stratagene, La Jolla, CA) in accordance with the manufacturer's instructions with the primer pairs S375Nfw (5′-AAATTGTAACGCACAATTTTAATTGTGGAGG-3′) and S375Nrv (5′-CCTCCACAATTAAAATTGTGCGTTACAATTT-3′), V255Efw (5′-GAATTAGGCCAGTAGAATCAACTCAACTGCT-3′) and V255Erv (5′-AGCAGTTGAGTTGATTCTACTGGCCTAATTC-3′), and A433Tfw (5′-CAGGAAGTAGGAAAAACAATGTATGCCCCTC-3′) and A433Trv (5′-GAGGGGCATACATTGTTTTTCCTACTTCCTG-3′), respectively.

Pseudovirus preparation. Portions, 5 μg of pSG3ΔEnv and 0.5 μg of pRSV-Rev (17), supplied by the NIH ARRRP, and a 4.5-μg portion of HIV-1_{IIIB} Env-expressing pCXN2 were cotransfected into 293T cells using the Effectene transfection reagent (Qiagen). At 48 h after transfection, the pseudovirus-containing supernatants were harvested, filtered through a 0.2-μm-pore-size filter, and stored at −80°C. The pseudovirus activities were measured with a luminescence assay using TZM-bl cells as previously described (28).

Single-round virus infection assay. A single-cycle infectivity assay was used to measure the neutralization of HIV-1_{IIIB} pseudoviruses as described previously (26, 28). Briefly, NBD-556, YYA-004, sCD4, 2G12, b12, RPA-T4, or 4C11 at various concentrations and a pseudovirus suspension corresponding to 100 $TCID_{50}$ were preincubated in the absence or presence of 1 μM NBD-556 for 15 min on ice. The virus-compound mixtures were added to TZM-bl cells, which had been seeded in a 96-well plate (1.5×10^4 cells/well) on the previous day. The cultures were incubated for 2 days at 37°C, washed with PBS, and lysed with lysis solution (Galacto-Star mammalian reporter gene assay system; ABI). After transfer of the cell lysates to luminometer plates, the β-galactosidase activity (in relative light units) in each well was measured by using 50-fold-diluted Galacto-Star substrate in a reaction buffer diluent (100 μl/well; ABI) in a TR717 microplate luminometer (ABI). The reduction in infectivity was determined by comparing the relative light units in the presence or absence of each compound and expressed as the percentage of neutralization. Each assay was repeated two to three times.

RESULTS

Anti-HIV-1 activities of sCD4, NBD-556, and YYA-004 for laboratory strains and primary HIV-1 isolates. Initially, we determined the inhibitory activities of sCD4, NBD-556, and YYA-004, which has a phenyl group instead of the *p*-chlorophenyl group of NBD-556 (Fig. 1), on the infection of PM1/CCR5 cells by different laboratory-adapted HIV-1 strains and different HIV-1 primary isolates of subtype B, including both X4 and R5 viruses, by using a previously reported method (33). sCD4 inhibited the laboratory-adapted HIV-1 strains HIV-1_{IIIB}, HIV-$1_{89.6}$, HIV-1_{BaL}, HIV-1_{SF162}, HIV-1_{JR-FL}, and HIV-1_{YU2} with IC_{50}s ranging from 0.26 to 6.1 μg/ml (Table 1). NBD-556 inhibited the X4 virus HIV-1_{IIIB} and dualtropic virus HIV-$1_{89.6}$ with IC_{50}s of 7.8 and 11.4 μM, respectively, but did not inhibit the R5 viruses HIV-1_{BaL}, HIV-1_{SF162}, HIV-1_{JR-FL}, and HIV-1_{YU2} with IC_{50}s of >30 μM. We also tested sCD4 and NBD-556 against the R5 primary isolates HIV-$1_{Pt.1}$, HIV-$1_{Pt.2}$, HIV-$1_{Pt.3}$, and HIV-$1_{Pt.4}$. sCD4 effectively inhibited all of the primary isolates at concentrations of 0.2 to 7.4 μg/ml. On the other hand, NBD-556 inhibited two of the four primary

TABLE 1. Inhibitory activities of sCD4 and NBD-556 toward infection by laboratory and primary strains of HIV-1

Virus	Subtype	Cell	Mean IC_{50}[a] ± SD		
			sCD4 (μg/ml)	NBD-556 (μM)	YYA-004 (μM)
Laboratory-adapted viruses					
X4					
HIV-1_{IIIB}	B	PM1/CCR5	0.26 ± 0.17	7.8 ± 2.6	>100
Dual					
HIV-$1_{89.6}$	B	PM1/CCR5	0.87 ± 0.09	11.4 ± 2.4	>100
R5					
HIV-1_{BaL}	B	PM1/CCR5	1.7 ± 0.28	>30	>100
HIV-1_{SF162}	B	PM1/CCR5	3.6 ± 0.64	>30	>100
HIV-1_{JR-FL}	B	PM1/CCR5	3.6 ± 0.71	>30	>100
HIV-1_{YU2}	B	PM1/CCR5	6.1 ± 2.00	>30	>100
Primary isolates					
R5					
HIV-$1_{Pt.1}$	B	PM1/CCR5	0.2 ± 0.04	3.6 ± 0.67	>100
HIV-$1_{Pt.2}$	B	PM1/CCR5	1.6 ± 0.21	>30	>100
HIV-$1_{Pt.3}$	B	PM1/CCR5	3.7 ± 0.42	11.8 ± 1.6	>100
HIV-$1_{Pt.4}$	B	PM1/CCR5	7.4 ± 1.30	>30	>100

[a] PM1/CCR5 cells (2×10^3) were exposed to 100 $TCID_{50}$ of each virus and then cultured in the presence of various concentrations of sCD4, NBD-556, or YYA-004 as indicated. The IC_{50}s were determined by using the MTT assay on day 7 of culture. All assays were conducted in duplicate, and the data shown represent the means derived from the results of two to three independent experiments. For NBD-556, CC_{50} = 140 μM; for YYA-004, CC_{50} = 350 μM. (The CC_{50} is the concentration for 50% cytotoxicity.)

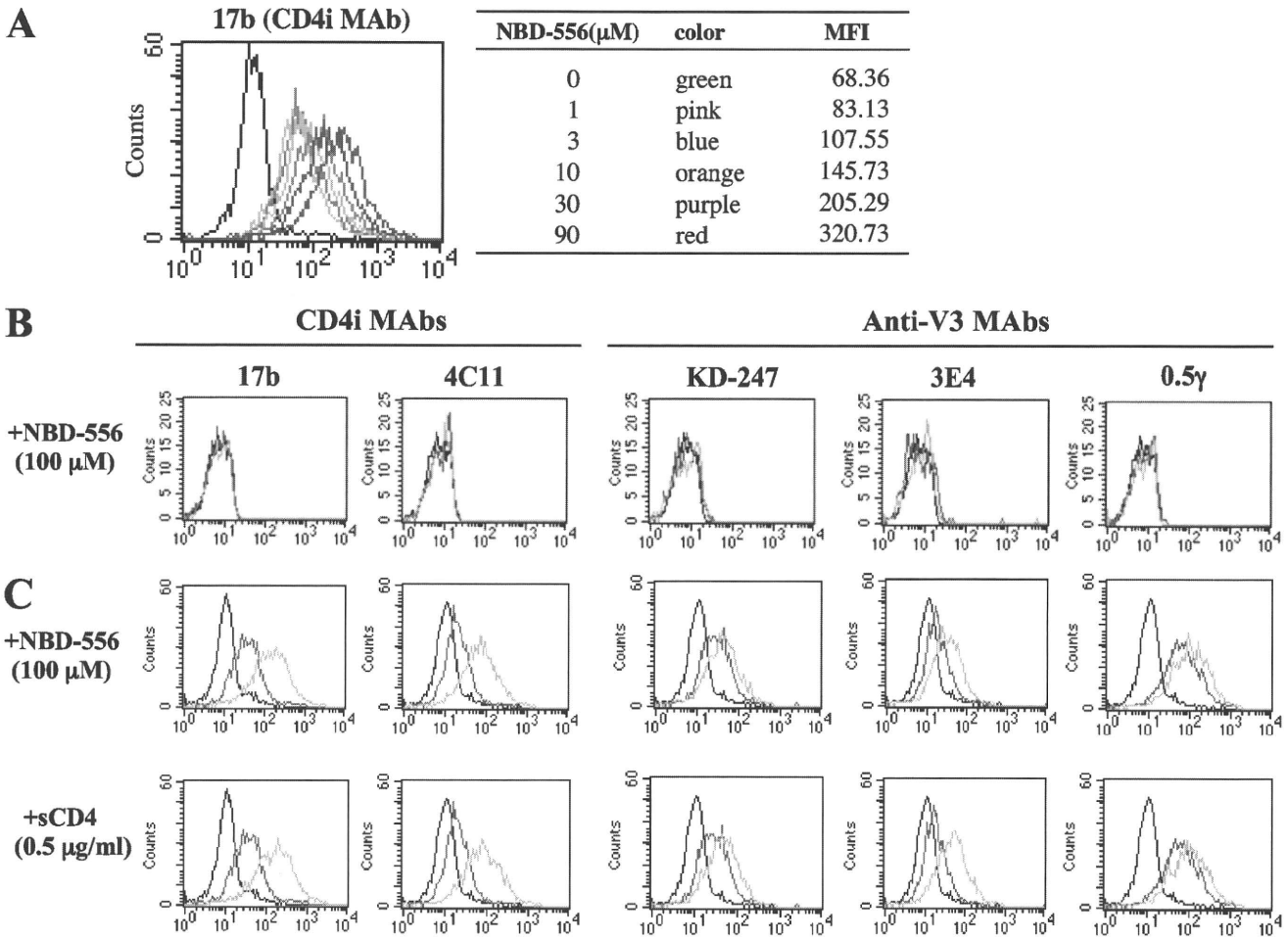

NBD-556(μM)	color	MFI
0	green	68.36
1	pink	83.13
3	blue	107.55
10	orange	145.73
30	purple	205.29
90	red	320.73

FIG. 2. Comparisons of MAb binding to cell surface-expressed gp120 with sCD4 and NBD-556. HIV-1_{JR-FL} chronically infected PM1 cells were preincubated with or without NBD-556 (A, 1 to 90 μM; C, 100 μM) or sCD4 (C, 0.5 μg/ml), and uninfected PM1 cells were also preincubated with or without NBD-556 (B, 100 μM) for 15 min, and then incubated with various anti-HIV-1 MAbs (17b, 4C11, KD-247, 3E4, and 0.5γ) at 4°C for 30 min. The cells were washed, and a fluorescein isothiocyanate-conjugated anti-human IgG was used for detection. (A) Color lines show the concentrations of NBD-556: green, 0 μM; pink, 1 μM; blue, 3 μM; orange, 10 μM; purple, 30 μM; and red, 90 μM. (B and C) Red line shows no preincubated with NBD-556 or sCD4. Blue line shows preincubated with NBD-556 or sCD4. Black line shows using a control IgG MAb.

isolates, HIV-$1_{Pt.1}$ and HIV-$1_{Pt.3}$, with IC_{50}s of 3.6 and 11.8 μM, respectively (Table 1). YYA-004 did not show significant anti-HIV activity against any of the strains tested up to a concentration of 100 μM. The *in vitro* cytotoxicities of NBD-556 and YYA-004 toward PM1/CCR5 cells used for the anti-HIV-1 infectivity studies were determined by using the MTT assay. The CC_{50} values of NBD-556 and YYA-004 toward PM1/CCR5 cells were 140 and 350 μM, respectively (Table 1).

Comparison of Ab binding to cell surface-expressed HIV-1_{JR-FL} Env with NBD-556 and sCD4. To compare the effect of NBD-556 with that of sCD4 with respect to the induction of conformational change in the trimeric gp120, the binding of CD4i MAbs (17b and 4C11) and anti-V3 MAbs (KD-247, 3E4, and 0.5γ) to cell surface-expressed Env proteins on HIV-1_{JR-FL} chronically infected PM1 cells was analyzed by fluorescence-activated cell sorting. Comparisons of the binding profiles of the Abs to the cell surfaces were carried out using the mean fluorescence intensity (MFI). The binding of CD4i MAb 17b increased gradually as the amount of the CD4-mimicking small compound NBD-556 increased from 0 to 90 μM (Fig. 2A, the MFI increased from 68.36 to 320.73). As shown in Fig. 2C, the binding of both CD4i MAbs 17b and 4C11 increased remarkably after pretreatment with 100 μM NBD-556 (the MFIs increased from 43.3 to 201.57 and from 24.43 to 96.06, respectively). Moreover, the binding of all of the anti-V3 MAbs—KD-247, 3E4, and 0.5γ—was enhanced by pretreatment with NBD-556 (the MFIs increased from 34.59 to 51.9, from 22.97 to 39.07, and from 86.61 to 145.08, respectively). sCD4 pretreatment of the Env-expressing cell surface also caused remarkable enhancement of the binding for not only the CD4i MAbs but also the three anti-V3 MAbs, similar to pretreatment with NBD-556. These results indicate that the CD4-mimicking compound NBD-556 can induce the conformational changes in gp120 that are caused by binding of sCD4.

Highly synergistic interactions of KD-247 combined with NBD-556. Both neutralizing anti-V3 MAb KD-247 and NBD-556 block the viral entry process, especially at the stage of the interaction between CD4 and gp120 (CD4-binding site). Each of these agents binds to either the V3 loop or the CD4 cavity. Furthermore, our previous observations suggested that neu-